UNIVERSITY OF CALIFORNIA, IRVINE

Development of Implantable Dual L-glutamate:GABA Sensors for Neuroscience Studies

DISSERTATION

submitted in partial satisfaction of the requirements
for the degree of

DOCTOR OF PHILOSOPHY

in Biomedical Engineering

by

Sung Sik Chu

Dissertation Committee:
Associate Professor Hung Cao, Chair
Chancellor's Professor Abraham Lee
Assistant Professor An Do

2023

DEDICATION

To my family,

Thank you for providing me with this great life with wonderful opportunities.

You are always my role models and the biggest motivation for me.

TABLE OF CONTENTS

LIST OF FIGURES

Page

Chapter 1:

Chapter 2:

Chapter 3:

Chapter 4:

ACKNOWLEDGEMENTS

I would like to thank Dr. Hung Cao for his guidance and support throughout my graduate studies at University of California Irvine. Dr. Cao not only guided me in the academic achievements but also, he supported me mentally throughout the whole journey so that I can finish my graduate studies. His passion towards science, especially for biomedical devices motivated me and his nourishing ideas helped me learn invaluable knowledge. Joining the HERO lab and working with Dr. Cao has been a wonderful experience and the best choice I made during my graduate years.

I would also like to thank my committee members, Professor Abraham Lee and Professor An Do. Thank you, Dr. Lee, for being the committee member that was present for all three of my milestones as a Chair for preliminary exam and as one of the committee members for others. Your thorough feedback on my preliminary exam helped me improve my presentations and critical thinking skills. Thank you, Dr. Do, for always supporting me and providing me the positive energy towards my experiments.

To the HERO lab, thank you all for being great lab mates and for the great memories we made in and outside the lab. To Dr. Paul Marsh, thank you for educating me in all the necessary skills required for my project. Also, thank you Crystal Han for starting the initial setup for this proposal together.

Lastly, I thank my family and friends for believing in me. Being on the other side of the world alone was tough, but I was able to finish this journey because of all your support. To all the Korean friends I made here, thank you for all the great memories we made and for always looking out after me. To all the BME friends, thank you for helping me adapt to the new environment and I enjoyed our study sessions in our first year. To my parents and my sister, I cannot thank you enough for all those empowering words that you provided every weekend during our calls and this accomplishment is not just mine but ours that we achieved.

I thank Springer Nature for permission to include copyrighted figures as part of my dissertation. I also thank Elsevier for permission to include Chapter Two of my dissertation, which was originally published in *Biosensors and Bioelectronics*. Financial support was provided by the NSF Grant NCS-1926818.

VITA

Sung Sik Chu

E D U C A T I O N

University of California, Irvine Irvine, CA
Doctor of Philosophy, Biomedical Engineering. GPA: 3.99 June 2023
Awards/Honors: Dean's Fellowship (2018 – 2019), Samueli Endowed Fellowship (Spring 2019)

Chung-Ang University Seoul, South Korea
Bachelor of Engineering, Biomedical Engineering. GPA:3.84 March 2018

R E L A T E D E X P E R I E N C E

HERO Lab, University of California Irvine Irvine, CA
Graduate Student Researcher June 2019 - present

Development of Implantable Dual L-glutamate:GABA Microsensors for Neuroscience Studies

- Designed MEMS and fabricated flexible microelectrode array using photolithography
- Modified surface of the sensor using electrochemical methods
- Characterized the surface of the sensor using SEM and EDX
- Investigated biocompatible materials for implantable biosensor
- Analyzed data for sensitivity, selectivity, and limit of detection (LOD)
- Performed *in vitro*, *ex vivo* (cell culture) and *in vivo* (rat brain) validation
- Reported highly sensitive, flexible dual L-glutamate and GABA microsensors for *in vivo* brain sensing

Development of Implantable Dual Glucose:Lactate Microsensors

- Fabricated flexible dual glucose and lactate electrochemical sensor for stroke study

BEST Lab, Chung-Ang University Seoul, South Korea
Undergraduate Student Researcher Dec 2015 – Aug 2018

Development of Highly Sensitive Dopamine Sensor Using 3D Porous Graphene Oxide/Gold Nanoparticle Composites

- Synthesized new 3D porous graphene oxide (pGO)/gold nanoparticle (GNP)/pGO composite on indium tin oxide (ITO) fabricated through ultrasonication
- Modified sensor surface using oxygen plasma and chemical silanization
- Performed electrochemical measurements (CV & amperometry) to analyze the sensor performance

Development of Conductive Hybrid Matrigel Layer for Electrochemical Detection of Human Embryonic Stem Cells

- Fabricated an electrochemical platform to monitor residual undifferentiated human pluripotent stem cells (hPSCs) for teratoma-free stem cell-based therapies
- Reported new composition of materials by mixing gold nanoparticles (GNPs) and branched arginyl-glycyl-aspartic acid (RGD) peptides in a Matrigel for higher cell adhesion and signal sensitivity
- Performed electrochemical detection (DPV) and reduced LOD from previously reported 72,000 human embryonic stem cells (hESCs) to 25,000 hESCs

Electrochemical Sensor for Precise Detection of Curcumin Cytotoxicity in Human Liver Cancer Cells

- Developed conductive cell culture platform for electrochemical drug cytotoxicity test with 3.71-fold higher sensitivity compared to conventional CCK-8 assay
- Modified the surface of the sensor using electrochemical deposition of GNPs and RGD peptides for higher sensitivity
- Cultured HepG2 cells on the electrochemical detection platform

TEACHING EXPERIENCE

UCI: BME 111 - Biomaterials 2023
Teaching Assistant

SELECTED PUBLICATIONS

- **Chu, S. S.**, Nguyen, H. A., Lin, D., Bhatti, M., Jones-Tinsley, C. E., Do, A. H., ... & Cao, H. (2022). Development of highly sensitive, flexible dual L-glutamate and GABA microsensors for *in vivo* brain sensing. Biosensors and Bioelectronics, 114941.
- **Chu, S. S**., Nguyen, H. A., Zhang, J., Tabassum, S., & Cao, H. (2022). Towards Multiplexed and Multimodal Biosensor Platforms in Real-Time Monitoring of Metabolic Disorders. Sensors, 22(14), 5200.
- Angeline, N., **Choo, S. S.**, Kim, C. H., Bhang, S. H., & Kim, T. H. (2021). Precise Electrical Detection of Curcumin Cytotoxicity in Human Liver Cancer Cells. BioChip Journal, 15(1), 52-60.
- Kim, D. S., Kang, E. S., Baek, S., **Choo, S. S**., Chung, Y. H., Lee, D., ... & Kim, T. H. (2018). Electrochemical detection of dopamine using periodic cylindrical gold nanoelectrode arrays. Scientific reports, 8(1), 1-10.
- Suhito, I. R., Angeline, N., **Choo, S. S.**, Woo, H. Y., Paik, T., Lee, T., & Kim, T. H. (2018). Nanobiosensing platforms for real-time and non-invasive monitoring of stem cell pluripotency and differentiation. Sensors, 18(9), 2755.
- **Choo, S. S.**, Kang, E. S., Song, I., Lee, D., Choi, J. W., & Kim, T. H. (2017). Electrochemical detection of dopamine using 3D porous graphene oxide/gold nanoparticle composites. Sensors, 17(4), 861.
- Jeong, H. C., **Choo, S. S.**, Kim, K. T., Hong, K. S., Moon, S. H., Cha, H. J., & Kim, T. H. (2017). Conductive hybrid matrigel layer to enhance electrochemical signals of human embryonic stem cells. Sensors and Actuators B: Chemical, 242, 224-230.

ABSTRACT OF THE DISSERTATION

Development of Implantable Dual L-glutamate:GABA Sensors for Neuroscience Studies

by

Sung Sik Chu

Doctor of Philosophy in Biomedical Engineering

University of California, Irvine, 2023

Professor Hung Cao, Chair

The imbalance between L-glutamate (L-glu) and Gamma-aminobutyric acid (GABA), the most abundant excitatory and inhibitory neurotransmitters, respectively, has been hypothesized to be related to various neurological disorders such as autism spectrum disorder, seizures, and epilepsy. Despite the importance of monitoring their balance, tracking the L-glutamate and Gamma-aminobutyric acid (GABA) levels real-time is very challenging. Currently, microdialysis is being widely used for this purpose and while it shows great sensitivity and selectivity, there's a several minutes of delay limited by diffusion and the probe used in the process is still very large, making it less feasible for measurements in local areas. Thus, electrochemical sensors have been the area of research to overcome these temporal and spatial resolution of microdialysis. With enzymatic and electrochemical reactions, it yields seconds of rapid response time and microfabrication technology allows several sensing points to be assembled in a few hundred micrometers allowing better spatial resolution.

Therefore, for the first half of this work, we have developed a highly sensitive electrochemical sensor for dual detection of L-glutamate and GABA. By electrochemical deposition of platinum nanoparticles, the overall active surface area was increased that led to higher sensitivity. Further, a self-referencing technique was adapted in order to achieve higher signal-to-noise ratio. Additionally, the sensor was fabricated using a flexible polyimide substrate for less brain damage along with easier handling compared to its ceramic counterparts. This dual L-glu:GABA sensor was validated in various conditions including *in vitro*, *ex vivo* with cell cultures and *in vivo* with anesthetized rodents. Furthermore, we tried improving its biocompatibility by exploring substitutional material for Ag/AgCl, a commonly used material for reference electrode in electrochemical systems. To replace Ag/AgCl, iridium oxide (IrOx) has been explored in terms of its biocompatibility and stability as a reference electrode. As a result, we were able to see IrOx's capability to replace Ag/AgCl for better biocompatibility in long term measurements *in vivo*. Overall, our dual L-glutamate:GABA electrochemical biosensor has its unique features to enable accurate, real-time, and long-term monitoring of the E:I balance *in vivo*. Improvements in various aspects of the sensor have been made along with its validation in multiple settings. This new tool is expected to aid investigations of neural mechanisms of normal brain function and various neurological disorders.

CHAPTER 1: INTRODUCTION AND BACKGROUND

1.1 Value of Electrochemical Biosensor for Neuroscience Studies

Neurotransmitters are chemical substances secreted at the end of a nerve fiber to affect another cell across a synapse and the binding of neurotransmitters results in either excitation or inhibition of the postsynaptic neuron. L-glutamate (Glu) and Gamma-aminobutyric acid (GABA) are the most abundant excitatory and inhibitory neurotransmitters in the central nervous system of mammals, respectively. Being the most abundant, these neurotransmitters are assumed to be involved in various neurological disorders including seizures, autism spectrum disorder, Parkinson's disease, etc [2-8]. Accordingly, recent studies hypothesized that not only the change in Glu and GABA levels individually but also the imbalance between the two could lead to developing a neurological disorder. We are especially interested in looking at the mechanism of this imbalance related to the early life sleep disruption (ELSD) and autistic behaviors that follows.

Autism spectrum disorder (ASD) is one of the serious childhood development disorders where the patient experiences difficulties in social interaction and communication [9]. While the number of autism patients keeps increasing throughout the years, the exact cause for the disorder has not yet been confirmed [10]. One of the hypothetical causes for the phenomenon is thought to be the imbalance between the amount of excitatory and inhibitory neurotransmitters in the brain. Some scientists speculate that ELSD is attributed to this imbalance that ultimately leads to ASD development [11-13]. To validate this hypothesis, a way to measure the amount of excitatory and inhibitory neurotransmitters real-time *in vivo* is highly in demand.

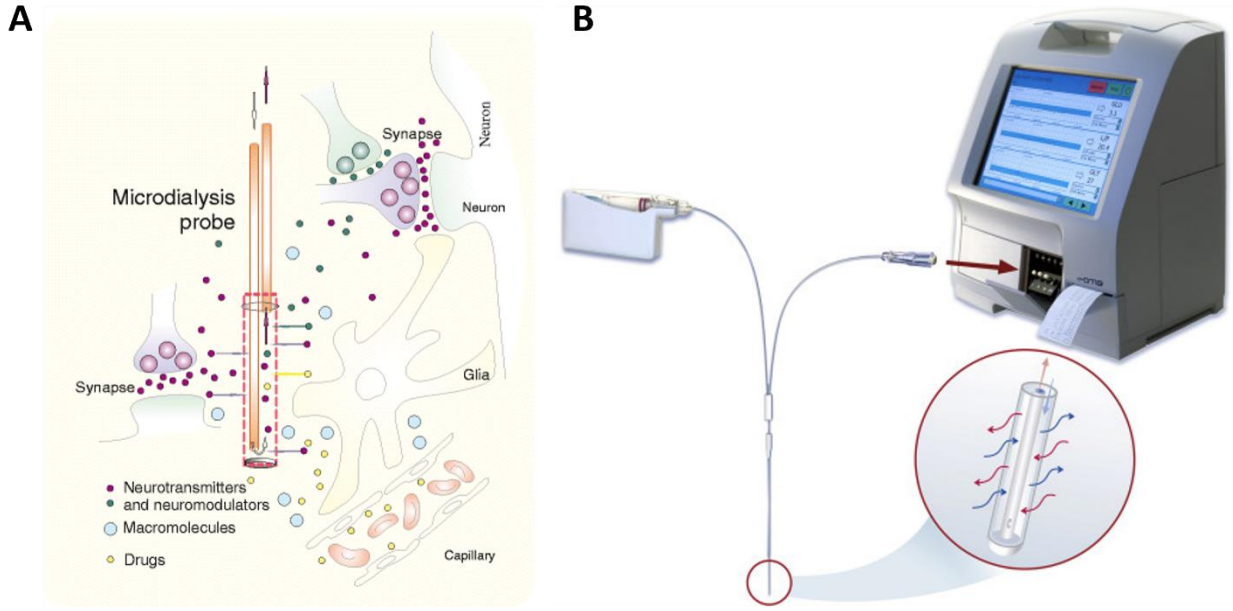

Figure 1.1 *Microdialysis. A. Interaction between different compartments of the microdialysis probe and neuronal tissue. Liquid flow inside the microdialysis probe allows diffusion of molecules via concentration gradient and pass through the probe membrane. B. Schematic depiction of microdialysis setup. Graphics adapted from [1]*

Currently, microdialysis is widely being used for this purpose where a small catheter is inserted to the measurement site and solutes of interest cross the semipermeable membrane from the concentration gradient (Figure 1.1.A) [14-16]. However, since the analytes must diffuse through the membrane first and then be collected at the external device for analysis, the temporal resolution for this technique is relatively poor to be used to study the mechanism of neurotransmitter release related to social behaviors [17, 18]. Also, the catheter that is being inserted goes far beyond several millimeters making it impossible to measure the neurotransmitters at a specific region of the brain, limiting its spatial resolution [19, 20]. On top of these drawbacks with its spatiotemporal resolution, microdialysis requires a big equipment to be tethered along with the catheter which limits the subject's mobility during the measurement hindering it from long-term monitoring (Figure 1.1.B). Alternatively, electrochemical sensors using

microelectrode arrays (MEAs) offer second-by-second detection with submillimeter spatial resolution within the brain [21-23]. Because neurotransmitters are released instantaneously when performing behavioral action, a method that can monitor this change in seconds needs to be implemented.

1.2 Motivation for the Dissertation

ASD refers to a cluster of childhood developmental disorders, where characteristics such as intellectual disability, difficulties in social interaction and communication, and repetitive behaviors are observed. According to the Centers for Disease Control and Prevention (CDC), one in every 59 children are diagnosed with ASD in the U.S. in 2018 [24]. While the prevalence of ASD keeps increasing throughout the years, the exact cause for the disorder is still yet to be identified. However, some of the pathological properties that have been observed in ASD include increased dendritic spine density on neurons, and reduced numbers of GABAergic interneurons in certain brain regions [25, 26]. Dendritic spines are small membranous protrusion from a neuron's dendrite that typically receives input form a single axon at the synapse, which expresses Glu receptors on its surface. And GABAergic interneurons are inhibitory neurons of the nervous system that play a vital role in neural circuitry and activity by the release of GABA. Thus, from the functions of dendritic spines and GABAergic interneurons, we can speculate that the common pathologies for ASD, increased dendritic spine density and reduced numbers of GABAergic interneurons, can lead to changes in Glu and GABA levels.

Then what causes these changes in pathologies for ASD patients? While several factors may take place, some researchers point to postnatal development [27, 28].

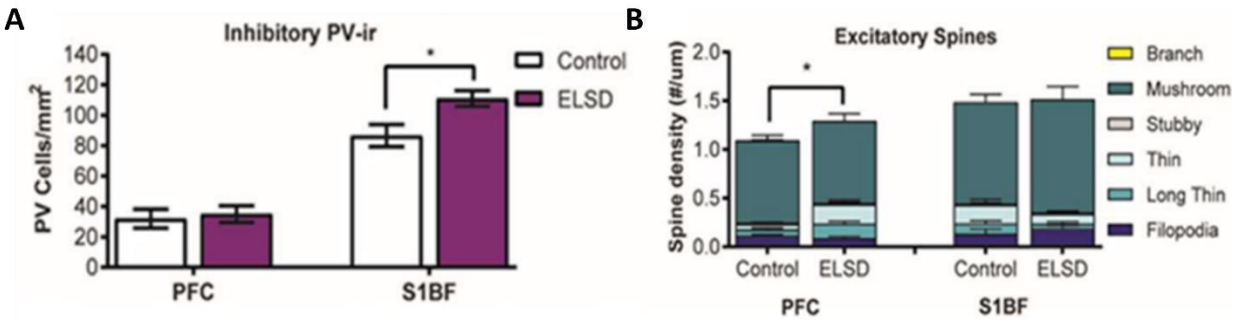

Figure 1.2 *(A) The increase of inhibitory parvalbumin interneurons in S1BF (p = 0.013) but not in prefrontal cortex (p > 0.7) after ELSD. (B) Increase density of excitatory synaptic growths in the PFC (p = 0.014) but not in S1BF (p > 0.9) after ELSD.*

Postnatal development period refers to when the time sleeping is at the maximum throughout the lifetime. And in this stage, the brain develops and tunes neural circuits to balance excitation and inhibition (E:I). Also, it has been proven in animal models that sleep deprivation leads to pathologies that are similar to that of the ones observed in children with ASD. In fact, our collaborator at OHSU have performed interesting research using immunohistology to test this hypothesis, where they induced disturbance to prairie vole pups during their sleep by placing the cage on an orbital shaker connected to a timer [29, 30]. The shaking was gentle enough and this method has been shown that it does not cause stress or interference with the normal nurture of the pups. Then they have analyzed the brain regions and compared it to the control animals which showed that the subjects with ELSD had increased parvalbumin in the somatosensory barrel field (S1BF) and increase population of dendritic spine around the prefrontal cortex (PFC) (Figure 1.2.A and 1.2.B). These results provide some evidence that ELSD can lead to changes in neurotransmitter levels. However, these were achieved after a certain period as the resulting value. It would be much more helpful if we could monitor the change in E:I balance in real-time, which is the main motivation for this project.

1.3 Principles of Electrochemistry for *in vivo* Neurotransmitter Detection

Electrochemistry refers to a field of chemistry that involves electron transfer reactions that are oxidation-reduction (redox) reactions, where electrons are transferred from one species to another. These either result in the generation of electricity or can be caused by imposing an electric current. In the case of electrochemical recordings *in vivo*, a microelectrode is implanted into the area of interest to read the signals generated by the chemical reactions, referred to as the working electrode (WE) [31]. Then a potential is applied versus a reference electrode (RE) through a potentiostat to oxidize or reduce the molecules of interest at the surface of the WE. And when molecules are oxidized, they release electrons which change the current at the recording region, where the change in current is proportional to the concentration of the molecules of interest.

Of various electrochemical methods, amperometry is widely used for *in vivo* recordings. This method measures current over time with a constant potential, which is suitable for looking at the concentration change of certain molecules over time. For neurotransmitter recordings in the brain, there are numerous neurotransmitters that coexist for neurons' signaling system [18]. And these neurotransmitters can be divided into either electroactive or non-electroactive [32]. In the case of electroactive molecules, when a potential is applied, the redox reaction takes place without any additional factors. Examples of these include ascorbic acid (vitamin C), dopamine, uric acid, etc. On the other hand, for non-electroactive molecules, additional mediators are required to convert them into a reporter molecule that is electroactive. And the examples of non-electroactive molecules in the brain are glucose, lactate, Glu, GABA, etc. Therefore, to measure Glu and GABA *in vivo*, an enzyme that acts as a mediator specific to the target neurotransmitters are

required to convert them into an electroactive molecule [33, 34]. And through the enzymatic reaction, the target neurotransmitter specifically binds to the enzyme, breaking down the neurotransmitters to its products, including hydrogen peroxide (H_2O_2). This H_2O_2 then further gets oxidized at the sensor's surface releasing electrons that leads to changes in current, which can be monitored through the electrochemical sensor.

1.4 Current Limitations

The validation of our hypothesis of ELSD leading to changes in E:I balance and resulting in ASD would be impossible to test in human subjects. While various methods such as liquid chromatographic (LC), capillary electrophoresis, potentiometric titrations, or fluorometric, are being investigated for *in vivo* detection of neurotransmitters, each method has its own limitations that need to be further addressed. As mentioned prior, one of the most widely used techniques for this purpose is microdialysis [1]. Although this technique allows good selectivity due to the use of semipermeable membranes and high sensitivity, the time required for the process is quite long and this limits the technique from being used for real-time measurements. Alternatively, electrochemical sensors are being investigated for their seconds of temporal and micrometers of spatial resolution.

However, the electrochemical sensors that have been reported so far also have some limitations in terms of low sensitivity, sensing mechanism, and biocompatibility. Currently, most of the sensors rely on using either silicon or ceramic as the sensor's substrate [35-38]. While it's easier to handle during the fabrication process and its rigidity can help with the sensor penetration process, it's expensive, prone to break and can even severely damage the brain from its stiffness. Furthermore, using a rigid substrate for long-term, continuous

monitoring of freely behaving animals may result in higher chance of electrode breaking due to the brittleness that comes from micrometers of size. Other limitations include the sensor's low sensitivity and the sensing mechanism which will further be explained in chapter 2.

1.5 Overview of the Dissertation

In this dissertation, we report an implantable electrochemical sensor for simultaneous detection of L-glutamate and GABA. Electrochemical sensors have been investigated in terms of neurotransmitter sensing owing to its advantages in simple fabrication process and real-time monitoring. This addresses the limitations of microdialysis in both spatial and temporal resolution. While multiple contributions to the field have been made by various groups, there is still room for improvement for *in vivo* neurotransmitter recordings.

First, the sensor's sensitivity and limit of detection need to be improved. The *in vivo* neurotransmitter signals that are collected by the electrochemical sensors reported previously are very low in pico-Amperes, which makes the signal easily influenced by the noises. These noises can be attributed from either the subject itself, such as within the brain or movement, or experimental setup, such as unstable ground or connection. Therefore, an effort needs to be made to enhance the signal quality for easier distinction of signal from the noise. In this dissertation, we have tried tackling the problem in several aspects. Initially, the optimal metal layer for the sensor was chosen for its oxidative properties to the reporter molecule, H_2O_2, for higher sensitivity. Several metals were compared for analysis where electrodes of gold (Au), silver (Ag), Copper (Cu), and platinum

(Pt) were made. Then with the optimal metal layer, we further increased the active electrode surface area by electrochemically depositing nanoparticles on the metal layer. In amperometry, the current detected by the WE are proportional to the active area of the electrode, which led us to explore methods for increasing the electroactive area of the sensor. Since the metal layer of the electrode is formed through electron beam resulting in a 2D layer, bringing it to a 3D configuration was thought of in order to increase the surface area through electrochemical deposition of metal nanoparticles. Additionally, to better enhance the signal to noise ratio (SNR), a self-referencing technique was adopted. As mentioned, there are numerous molecules that can possibly create electrical signal when potential is applied in the brain. The enzymes for the target neurotransmitter provide specificity towards Glu and GABA, but the signal generated from other electroactive molecules can still be read through the sensors. To address this issue, a self-referencing technique is incorporated into our sensor. Basically, we have fabricated a self-referencing pad in proximity to the actual sensing pad that can record all the noises, which the self-referencing signal can later be subtracted from the sensing signal to leave out only the target neurotransmitter signals. This eliminates the noises that can be caused by either the electroactive molecules in the target region or from the environment, enhancing the SNR of our sensor.

Second, the sensor's biocompatibility had to be considered for the goal of long-term measurements *in vivo*. There are multiple aspects of the sensor that affect its biocompatibility. For example, damage in brain tissue is inevitable for implantable sensors where the sensor is penetrating the brain to reach the target area of measurement. However, reducing the area of damage and the force exerted during the implantation can

be some things that can be addressed. The approach that we took was to minimize the size of the sensor by utilizing the optimal orientation of the sensing pads while using a high precision laser cutting system to rule out the excessive areas that can be left after the cutting process. To reduce the force exerted during implantation, a flexible substrate was chosen instead of previously reported rigid ones to hopefully alleviate the damage caused during the process and several designs for the electrode tip was compared for minimal scarring at the onset of initial penetration. Furthermore, on top of the mechanical aspects, chemical biocompatibility was addressed by exploring substitutional materials for RE. A typical RE used for *in vivo* electrochemical sensing is made of silver/silver chloride (Ag/AgCl). REs of Ag/AgCl wire have been widely used for *in vivo* electrochemical recordings owing to its reduction in terms of great stability. However, multiple studies have pointed out the issues regarding Ag/AgCl's biocompatibility. Therefore, a new material was explored as a substitute that can match the stability of Ag/AgCl while providing higher biocompatibility.

With above mentioned technical improvements of our sensor, the platform was tested in various settings for validation. Initially, the Glu:GABA sensor was tested *in vitro* in a laboratory setting by inducing neurotransmitter concentration changes in a beaker. The features of the sensor explored *in vitro* included sensitivity, selectivity, limit of detection, flexibility, longevity, biocompatibility, etc. After confirming the superior capability of our sensor *in vitro*, we further moved on to testing its performance *ex vivo* with neuronal cells. Here, a neuronal cell culture was cultivated for months for proper differentiation and a chemical was introduced for stimulation. With contact, our sensor was able to pick up the consecutive increase in current which correlates to the change in target neurotransmitter

concentration. Finally, the last step of validation we performed before long-term measurements *in vivo* was an *in vivo* experiment with anesthetized animal models. Similar to *ex vivo*, chemical stimulation was induced with an injection pump near the sensor implantation site, and we were able to observe the current increases following neuronal stimulation with our sensor. Likewise, the Glu:GABA sensor reported here has been vigorously validated for the goal of long-term *in vivo* recordings.

CHATPER 2: DEVELOPMENT OF HIGHLY SENSITIVE, FLEXIBLE DUAL L-GLUTAMATE AND GABA MICROSENSORS FOR *IN VIVO* BRAIN SENSING

Sung Sik Chu[1], Anh H. Nguyen[2], Derrick Lin[3], Mehwish Bhatti[4], Carolyn E. Jones-Tinsley[5], An Hong Do[3], Ron D. Frostig[1,4], Zoran Nenadic[1], Miranda M. Lim[5], Hung Cao[1,2,6]

Affiliation

[1]Department of Biomedical Engineering, University of California Irvine, CA, 92697, USA

[2]Department of Electrical Engineering and Computer Sciences, University of California Irvine, 92697, CA, USA

[3]Department of Neurology, University of California Irvine, CA, 92697, USA

[4]Department of Neurobiology and Behavior, University of California, CA, 92697, USA

[5]VA Portland Health Care System; Department of Neurology, Oregon Health and Science University, OR, 97239, USA

[6]Department of Anatomy and Neurobiology, University of California Irvine, CA, 92697, USA

[7]Center for Neural Circuit Mapping, University of California Irvine, CA, 92697, USA

[8]Department of Computer Science, University of California Irvine, CA, 92697, USA

2.1 Abstract

Real-time tracking of neurotransmitter levels *in vivo* has been technically challenging due to the low spatiotemporal resolution of current methods. Since the imbalance of cortical excitation / inhibition (E:I) ratios are associated with a variety of neurological disorders, accurate monitoring of excitatory and inhibitory neurotransmitter levels is crucial for investigating the underlying neural mechanisms of these conditions. Specifically, levels of the excitatory neurotransmitter L-glutamate, and the inhibitory neurotransmitter GABA, are assumed to play critical roles in the E:I balance. Therefore, in this work, a flexible electrochemical microsensor is developed for real-time simultaneous detection of L-glutamate and GABA. The flexible polyimide substrate was used for easier handling during implantation and measurement, along with less brain damage. Further, by electrochemically depositing platinum black nanostructures on the sensor's surface, the active surface area was enhanced for higher sensitivity. This dual neurotransmitter sensor probe was validated under various settings for its performance, including *in vitro*, *ex vivo* tests with glutamatergic neuronal cells and *in vivo* tests with anesthetized rats. Additionally, the sensor's performance has been further investigated in terms of longevity. Overall, our dual L-glutamate:GABA sensor microprobe has its unique features to enable accurate, real-time, and long-term monitoring of the E:I balance *in vivo*. Thus, this new tool should aid investigations of neural mechanisms of normal brain function and various neurological disorders.

Keywords: L-glutamate, GABA, electrochemical sensor, platinum black, microelectrode array, dual sensing

2.2 Introduction

L-glutamate (Glu) and gamma-aminobutyric acid (GABA) are the most abundant excitatory and inhibitory neurotransmitters in the central nervous system of mammals, respectively. They are assumed to be involved in various neurological disorders including seizures, trauma, and autism spectrum disorder (ASD) [39-42]. These conditions affect vast amount of people worldwide and specifically for ASD, while one in 44 children were diagnosed with ASD [43], the cause for the disorder remains unsolved. However, recent studies indicate that the change in excitatory and inhibitory neurotransmitters might be related to these disorders. Moreover, the relevant parameters proposed are not only the changes in neurotransmitter levels individually but also in excitatory: inhibitory (E:I) neurotransmitter balance [44, 45]. For ASD, recent findings discovered specific brain pathology associated with the E:I imbalance, such as overgrowth of dendritic spines that can lead to increased glutamatergic excitation and reduced numbers of GABAergic interneurons [46-48]. This indicates the possibility of E:I imbalance in ASD patients and therefore, an efficient and reliable way to measure the amount of Glu and GABA *in vivo*, real time is highly in demand. Microdialysis has been commonly used for measuring neurotransmitters *in vivo*, in which a small catheter is inserted into the measurement site and solutes of interest cross the semipermeable membrane due to the concentration difference [49, 50]. However, since the analyte must diffuse through the membrane before being collected for analysis, the temporal resolution for this technique is very low to be used for studying the mechanism of neurotransmitter release related to social behaviors [51, 52]. In addition, the spatial resolution is limited by the size of the catheter required. Alternatively, electrochemical sensors using microelectrode arrays (MEAs) have been

gaining attention for their second-by-second detection with submillimeter spatial resolution within the brain [31].

To date, many groups have reported electrochemical neurotransmitter sensors for various molecules, including dopamine, acetylcholine, Glu, and GABA, just to name a few [53-56]. Specifically, for Glu and GABA, enzyme-based sensors targeting each single neurotransmitter were developed in depth [57-59]. However, for dual sensing of Glu and GABA for monitoring E:I balance, there have been only a few. The main reason for this is that for GABase (the enzyme used for GABA sensors) to react with GABA, a precursor namely alpha-ketoglutarate (α-keto), is needed to be introduced externally. But since the discovery of the fact that α-keto is actually one of the products from the Glu reaction, few groups have started reporting a dual Glu:GABA sensor without the need for external α-keto [60-62]. As shown in Fig. 2.1, the α-keto required for the GABA reaction to occur can be replenished by the Glu reaction and the final reporting molecule, H_2O_2, gets oxidized on the

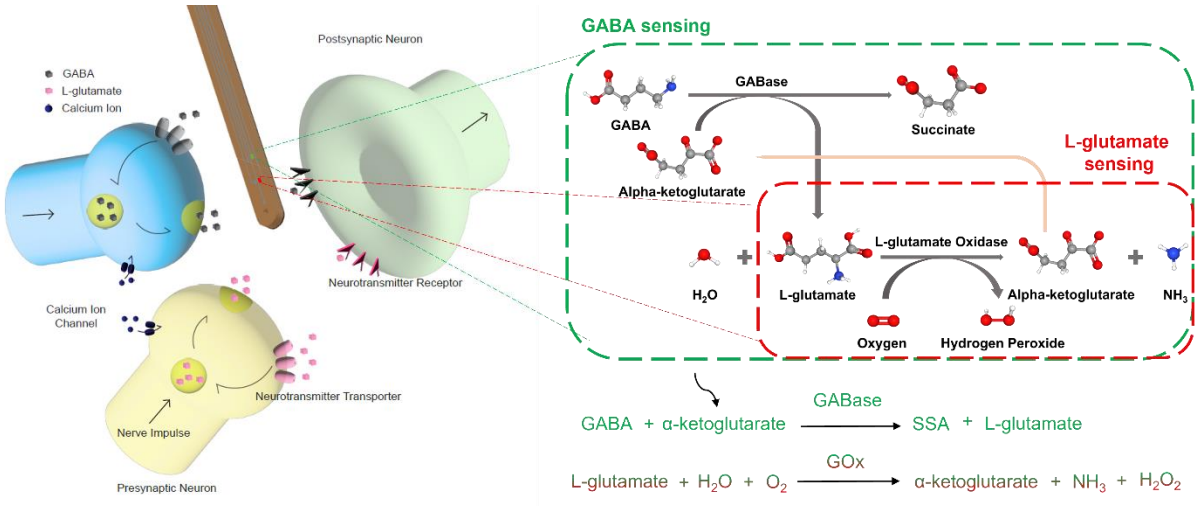

Figure 2.1. *Schematic diagram for L-glutamate and GABA sensing. The dual L-gluatmate:GABA sensor detects the neurotransmitters released to the extracellular space through specific enzymatic reactions. The alpha-ketoglutarate required for GABase reaction is supplemented via the L-glutamate oxidase reaction, making dual sensing possible without the need for any external molecules.*

sensor's surface. Nevertheless, the dual Glu:GABA sensors reported so far still possess several drawbacks to be addressed for improvement for reliable real-time *in vivo* measurements [61-64].

First, the previously reported dual neurotransmitter sensors utilized rigid substrates such as ceramic or silicon. However, because of the sensor's small dimensions, it is prone to break during implantation and this brittleness makes the sensors challenging to handle throughout the neurotransmitter monitoring process. Furthermore, detection in 2D platforms such as in cell cultures is not feasible since cell cultures typically does not provide enough depth for the sensor to be inserted. Another drawback of the previously reported dual neurotransmitter sensors is that the sensing surface of the sensors are made of bare platinum (Pt). This 2D surface holds a low active surface area, which is proportional with the sensory output (in ampere-A), in tens of pA. This calls for a strategy to achieve higher sensitivity to better distinguish the small amount of neurotransmitter level changes. To address these limitations, we propose to utilize flexible substrate for handling and to form nanostructures on the sensing surface to enhance the performance.

In this section, we introduce a flexible integrative dual Glu:GABA sensor with high sensitivity which can support a variety of neuroscience studies. To improve the performance, the biosensor was fabricated on a flexible polyimide substrate and platinum-black (Pt-black) nanostructures were electro-deposited to increase the active surface area. By providing more space for the molecules to react on, the overall current increases allowing enhanced sensitivity. An additional unique feature discussed in this section is longevity enhancement. With multiple updated features, the implantable dual Glu:GABA

neurotransmitter sensor was validated *in vitro*, *ex vivo* and *in vivo,* showing promising results to be further deployed for neuroscience studies.

2.3 Materials and Methods

2.3.1 Materials

Phosphate buffered saline (10X PBS), glutaraldehyde, and 30% hydrogen peroxide (H_2O_2) were purchased from Thermo Fisher Scientific (Waltham, MA). 97+% L-glutamic acid monopotassium salt monohydrate, 99.9% dihydrogen hexachloroplatinate(IV) hydrate hydrate, 99% dopamine hydrochloride (DA), and 97% bovine serum albumin (BSA) were purchased from Alfa Aesar (Haverhill, MA). L-ascorbic acid (AA), 99% m-phenylenediamine dihydrochloride (mPD), 98% potassium ferricyanide, and 99+% gamma-aminobutyric acid (GABA) was purchased from Acros Organics (Fair Lawn, NJ) and glutamate oxidase (GOx) from US Biological Life Science (Swampscott, MA). GABase and sodium pentobarbital were purchased from Sigma Aldrich (St. Louis, MO). Isoflurane was from Pivetal (Loveland, CO), and atropine sulfate was from Vedco (Saint Joseph, MO).

2.3.2 Microelectrode Array Design and Fabrication

The samples were first fabricated at University of California Irvine's Integrated Nanosystems Research Facility (INRF). Flexible 125-µm-thick polyimide films were cleaned with acetone, isopropyl alcohol (IPA) and deionized water (DI water) sequentially to remove any organic particles that might be present on its surface and dried with nitrogen gas. Then negative resist, NR9, was spin-coated on top of the polyimide followed by an ultraviolet (UV) light exposure to pattern the electrode layer. Onto the pattern, 20 nm of

Metal	Voltage (kV)	Current (mA)	Thickness (nm)	Deposition Rate (Å/s)
Chromium (Cr)	7.3	20	20	0.7 – 1.0
Gold (Au)	7.3	60	200	0.8 – 1.0
Platinum (Pt)	7.3	160	200	0.8 – 1.2

Figure 2.2 *Conditions for electron beam deposition.*

chromium (Cr) and 200 nm of either gold (Au) or platinum (Pt), were deposited with electron beam evaporator following the conditions listed in Fig. 2.2. Cr serves as an adhesion layer for platinum to adhere to the polyimide substrate. Then the traces and the pads were defined using a lift-off process, where an inverse pattern of sacrificial layer (NR9) was patterned before the metal deposition and lifted-off after the electron beam, leaving the target material only in the regions with direct contact. Afterwards, a barrier layer was made with SU-8 2000 to separate the sensing pads from the connecting traces. With heating and developing, the initial form of the sensor was obtained in a batch within 4-inch circular polymer samples (Figure 2.3), where it was sent to LASEA Inc. (El Cajon, CA)

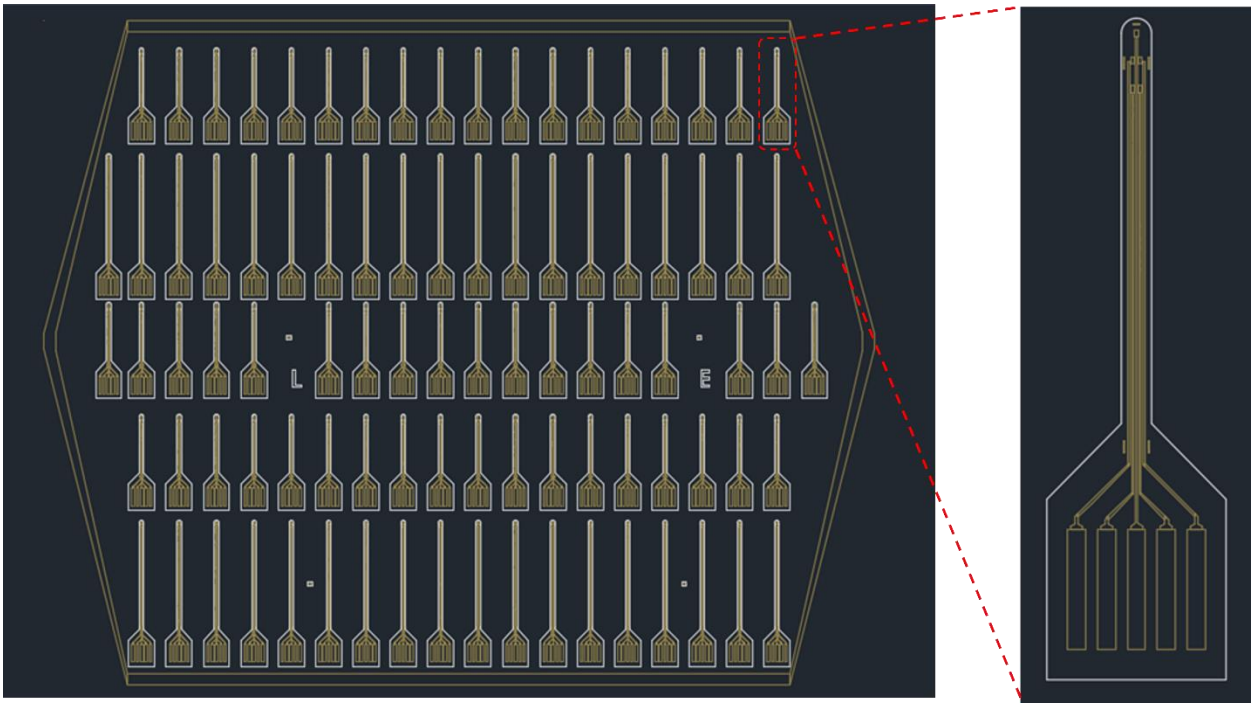

Figure 2.3 *CAD design for the batch of sensors. Right figure depicts the orientation of a single probe*

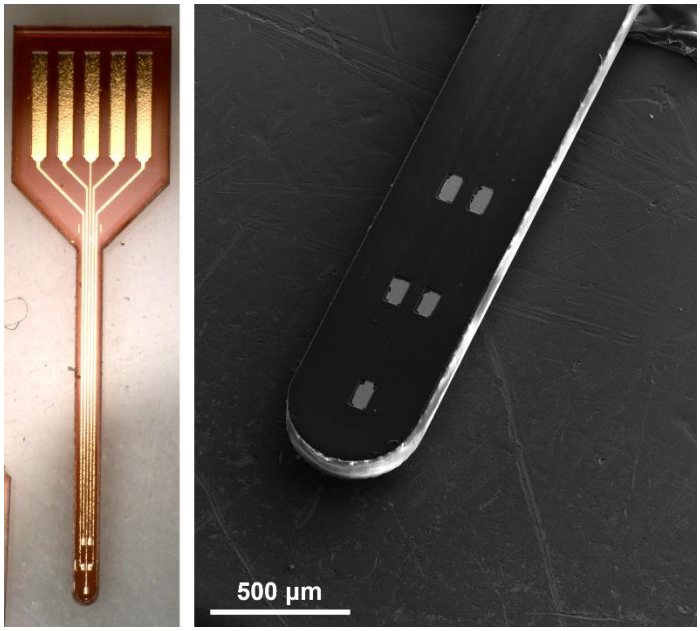

Figure 2.4 *The dual L-glutamate:GABA sensor probe after laser cutting (left) and the scanning electron microscopy (SEM) image of the tip (right). The 5 electrodes have a size of 50 µm × 100 µm, and the width of the probe shaft is 495 µm.*

for laser cutting process into single probes. The final form of the sensor after laser-cutting has a width of 495 µm and consists of five 50 µm × 100 µm pads (Figure 2.4), where the one in the middle is for pseudo-referencing, two on the right each refers to Glu and GABA sensing, and the two placed across from them are the self-referencing pads for the two neurotransmitters.

2.3.3 Surface Modification for Neurotransmitter Detection

For the electrodeposition of Pt nanostructures (Pt-black), first, 0.01-M chloroplatinic acid was made by dissolving chloroplatinic acid hydrate ($H_2PtCl_6 \cdot H_2O$) in DI water. Then potential ranging from -0.4 to +0.8 V v.s. a Ag/AgCl reference electrode was cycled with a scan rate of 50 mV/s for 10 cycles. A commercial potentiostat from CH Instruments was used (700 E, CH Instruments, Austin, TX) for the process and once the electrodeposition was accomplished, the sensors were rinsed with DI water and kept in air to dry before enzyme deposition.

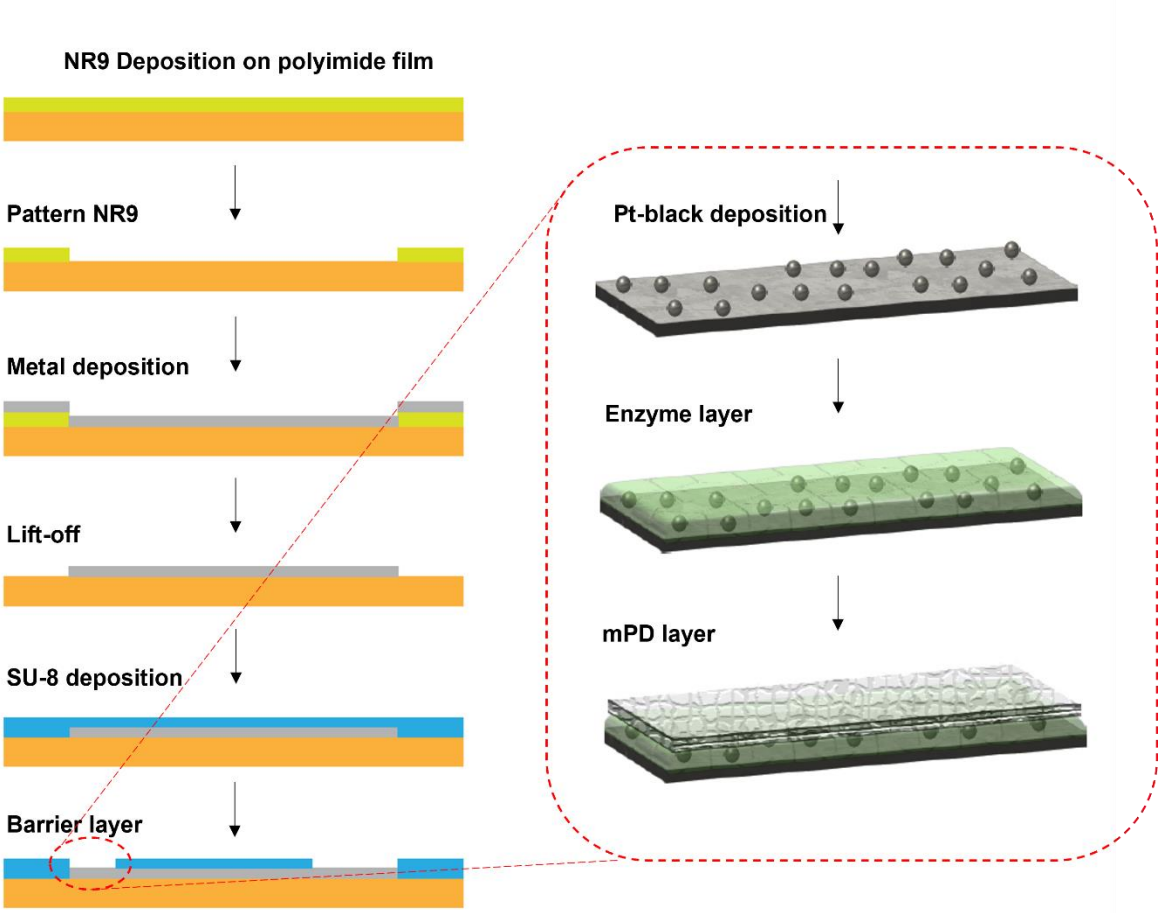

Figure 2.5 *Overall fabrication process of the sensor.*

Next, enzymes of interest were deposited on the sensing electrodes. First, 10 mg of BSA was dissolved in 985 µl of DI water followed by mixing 5 µl of glutaraldehyde into the BSA solution as a crosslinking agent. After inverting it manually 5 times, the solution was left at room temperature for 5 minutes for BSA to bind to one of the arms of glutaraldehyde. Meanwhile, the aliquoted enzymes stored in -80℃ were brought out to room temperature for thawing. Depending on the target neurotransmitter, either 0.5 µl of GOx (1U/1µl) or 0.5 µl of the GOx and 0.5 ul of the GABase (1U/1µl) were mixed with the BSA solution to make a total volume of 5 µl, where the amine groups of the enzymes bound to the other arm of glutaraldehyde. As for the mixtures applied on the self-referencing pads, the composition of solutions was the same except for the lack of enzymes for the

target neurotransmitter. In short, the self-referencing pad for Glu lacked GOx and for GABA lacked GABase. Once the solution was ready, the probes were placed under a stereotactic microscope for enzyme immobilization. Using 50 µl Hamilton's syringe, the enzymatic solution was drawn and manually deposited on the sensing pads of interest. For each pad, a total of 3 applications were made by drop casting the solution (approximately 0.05 µl/drop). Between each application, one minute interval was given for the solution to settle and once all the deposition has been completed, the probes were stored in the refrigerator at 4°C for at least 2 days for curing.

Lastly, an exclusion layer was formed on the surface for the sensor's selectivity. mPD, known to block the interferent molecules via size exclusion once polymerized, was adapted to repel other electroactive molecules that are present in brain and cause interference, such as AA and DA [65, 66]. A solution of 0.05 M PBS was deoxygenated by purging with nitrogen gas for 20 min followed by dissolving mPD to make the final concentration of 5 mM. Inside a fume hood, the enzyme deposited probes were immersed in the mPD solution and a potential between +0.2 to +0.8 V vs a Ag/AgCl reference electrode was cycled for 15 min. Once the deposition was done, the probes were rinsed with DI water and kept at 4°C for at least 24 hours before calibration. The overall sensor fabrication process is shown in Figure 2.5.

2.3.4 Characterization and Calibration

To quantify the increase in the sensor's active surface area through Pt-black deposition, Randles-Sevcik equation was used. This equation is commonly used to describe the effect of scan rate on the peak current, but it also relates the peak current with the electrode surface area [67]. Assuming room temperature:

$$i_p = (2.69 \times 10^5) n^{\frac{3}{2}} A D^{\frac{1}{2}} v^{\frac{1}{2}} C \quad (1)$$

where i_p is the peak current, n is the number of electrons transferred in the redox reaction (1 in this case), A is the electrode area in cm^2, D is the diffusion coefficient in cm^2/s, C is the concentration in mol/cm^3, and v is the scan rate in V/sec. The peaks of the waveform were calculated by using $K_3Fe(CN)_6$ as the redox couple for cyclic voltammetry. 5 mM of $K_3Fe(CN)_6$ in 0.1 M KCl was prepared and the probes were immersed in the solution. With a scan rate of 50 mV/s, potential between -0.2 to +0.6 V v.s. a Ag/AgCl reference electrode was cycled. From the resulting cyclic voltammogram, the peaks of the current were extracted and substituted into the equation to calculate the active surface area.

For the sensor's performance validation, a multichannel potentiostat from Pinnacle Technology Inc. (8102-N, Lawrence, KS) was used. A solution of either 1X PBS (for Glu) or 1 mM alpha-ketoglutarate (for GABA) was placed onto a hot plate to provide 37°C. Then the probes were immersed into the solution while applying +0.7 V against a Ag/AgCl reference electrode (RE) with constant magnetic stirring for uniform diffusion. Various known concentrations of Glu and GABA were dropped into the solution to achieve the sensitivity plot and additional molecules such as AA, DA, and H_2O_2 were introduced to test for selectivity. The limit of detection (LOD) was calculated by dividing 3 times the standard deviation of the baseline by the least squares slope.

2.3.5 *Ex vivo* Experiments

For sensor validation with glutamatergic neuronal cells, the cells were prepared by derivation from human induced pluripotent stem cells (iPSCs). iPSCs were first cultured on Matrigel coated microplates and differentiated to neural progenitor cells (NPCs) for three

weeks, using a commercial differentiation medium based on dual-SMAD inhibition (Neural Induction Medium, StemCell Technologies). Afterwards, NPCs were differentiated into glutamatergic neurons using neural differentiation medium (NDM; composed of neurobasal medium, 2% B-27, 200 µM ascorbic acid, and 1% Glutamax, Gibco) for 10 days at a 70% confluency. Finally, human iPSC derived astrocytes were mixed with the NPCs to establish a stable long term monolayer co-culture. Note that differentiation of human iPSCs to astrocytes was undertaken following the method from Serio et al., including exposure of NPCs to leukemia inhibitory factor (LIF), followed by fibroblast growth factor (FGF2), and ciliary neurotrophic factor (CNTF) over a 3-month period. After mixing astrocytes and the partially differentiated NPCs, differentiation of the NPCs into glutamatergic neurons continued for an additional 20 days using NDM supplemented with 1% N2 (Gibco). Subsequently, the neuron-astrocyte co-culture was maintained in NDM with 1% N2 for at least a month before they were used for glutamate activity measurements.

To maintain the neuronal cell's activity during the measurement, artificial cerebrospinal fluid (aCSF) was prepared. Chemicals were mixed to obtain the final composition of 125 mM NaCl, 26 mM $NaHCO_3$, 1.25 mM NaH_2PO_4, 4 mM glucose, 3 mM KCl, 1 mM $MgCl_2$, and 2 mM $CaCl_2$ in DI water. Once evenly mixed, the solution was filtered with 0.22 µm filter apparatus to filter out any biological debris and was stored in 4°C until further use.

At the day of the experiment, neurotransmitter sensors were validated *in vitro* prior to *ex vivo* testing and all the solutions required for the experiment was put into a water bath to match 37°C before use. Cells were placed on a hot plate to maintain a constant temperature of 37°C and were washed twice with aCSF after removing the culture medium.

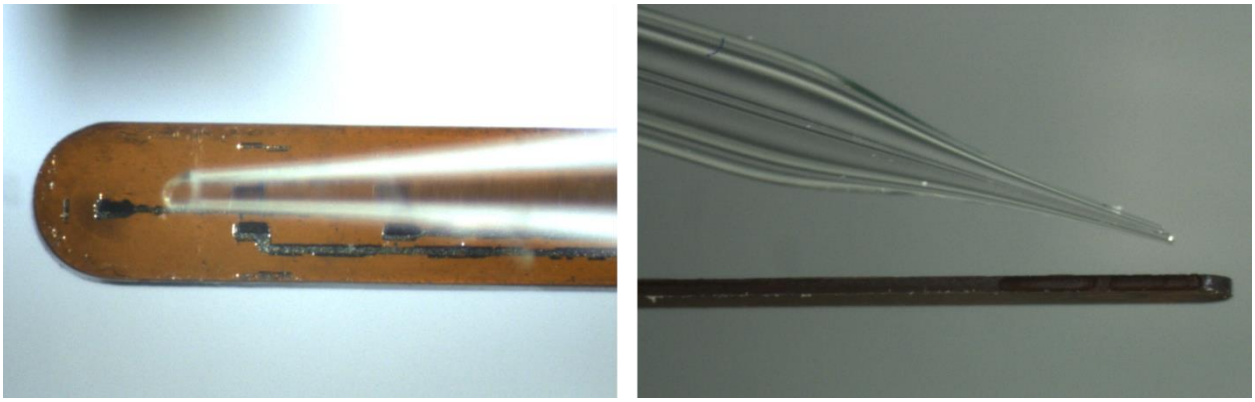

Figure 2.6 *Image of the micropipette attached along with the dual L-glutamate:GABA sensor for KCl stimulation. The top view is on the left while the right panel shows the side view.*

With the cells in aCSF, the neurotransmitter sensor and a AgCl silver pseudo-RE were placed in proximity using stereotaxic holders. Constant potential of +0.7 V was applied with the 8102-N multichannel potentiostat from Pinnacle Inc., and 15 to 20 minutes of stabilization period was given. Once ready for recording, filtered 70 mM KCl with a composition of 70 mM KCl, 79 mM NaCl and 2.5 mM $CaCl_2$ in DI water (pH 7.4) was locally applied to stimulate the glutamatergic neurons and current changes related to this chemical stimulation were observed.

2.3.6 *In vivo* Experiments

All animal protocols were reviewed and approved by Institutional Animal Care and Use Committee (IACUC) protocol (# AUP-21-079, University of California, Irvine). Male Sprague-Dawley rats were used for this study. Rats were anesthetized with 4% isoflurane until a toe-pinch reflex is no longer present. A bolus of sodium pentobarbital (55 mg/kg, b.w.) was then injected interperitoneally. Atropine sulphate (0.05 mg/kg, b.w.) injection was followed to help reduce the secretions to facilitate breathing. Then, a rectal probe was inserted to monitor and maintain the rat's body temperature using heating blanket's feedback system. To expose the recording site, a midline incision was made and after

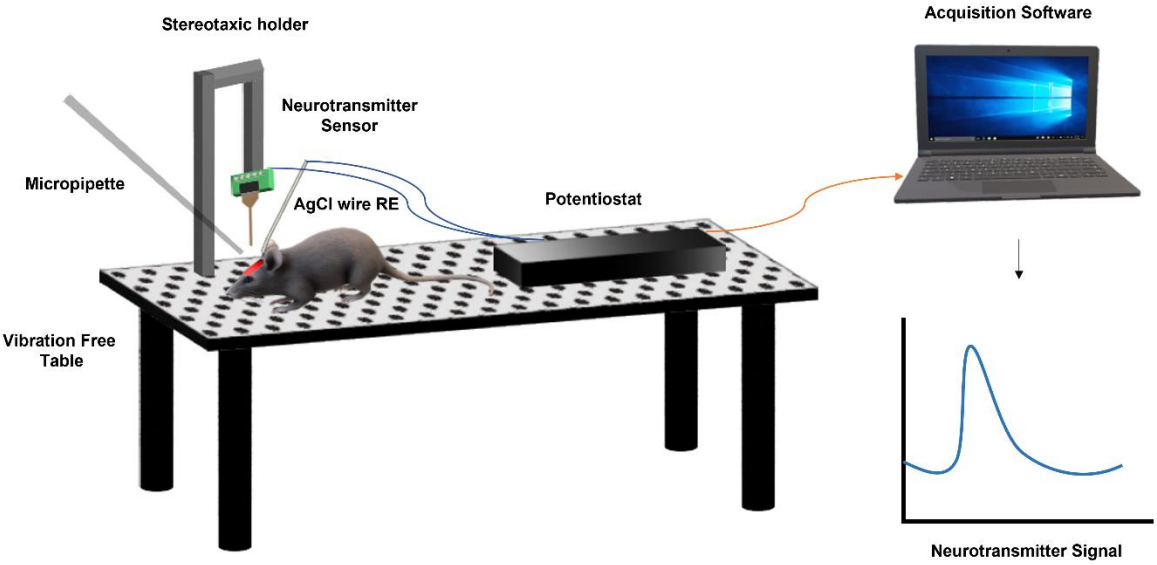

Figure 2.7 *Schematic of in vivo setup. Briefly, using a stereotaxic holder, the dual Glu:GABA sensor was lowered to the cortical layer 4 of the rat's primary barrel cortex and potential was applied against a AgCl silver wire pseudo-RE. For stimulation, through glass micropipette attached to the sensor platform, local injection of 70 mM KCL was performed using a syringe pump. Real-time response and changes in current was recorded through the acquisition system.*

resection of the underneath tissue craniotomy and durotomy of 2 mm × 2 mm were made over the rat's primary somatosensory cortex. The dual Glu:GABA sensor was lowered in the cortical layer 4 of the rat's primary barrel cortex and a constant potential of +0.7 V was applied against a AgCl silver wire pseudo-RE. During the recording, the rats were supplemented with sodium pentobarbital (14 mg/kg, b.w.) every 45 minutes or as required to maintain steady anesthesia. After a stabilization period of 30 to 40 minutes for baseline establishment, through glass micropipettes that were attached to the sensor platform (Figure 2.6), local injection of 70 mM KCl was given to stimulate brain extracellular space using Microinjection Syringe Pump (World Precision Instruments, Sarasota, FL). For the recordings, the Tethered Mouse System from Pinnacle Technology Inc. (8400-K1, Lawrence, KS) was used. A simplified schematic of the setup is shown in Figure 2.7.

2.4 Results and Discussion

2.4.1 Material Optimization for Oxidative Properties

To enhance the sensitivity our dual Glu:GABA amperometric sensors, one of the approaches that we took was to increase the active surface area based on the Cottrell equation [68]:

$$i = \frac{nFAc_0\sqrt{D}}{\sqrt{\pi t}} \qquad (2)$$

where i is the current (A); n is the number of electrons transferred; F is the Faraday constant (F = 96,487 C·mol^{-1}); A is the surface area of planar electrode (cm^2); c_0 is the initial concentration of the analyte (mol·mL^{-1}); D is the diffusion coefficient (cm^2·s^{-1}); t is the time elapsed since the potential was applied (s). Looking at the equation, since the current is proportional to the surface area of the planar electrode, increasing the surface area of the electrode can be a straightforward approach to increase the output current. Hence, to

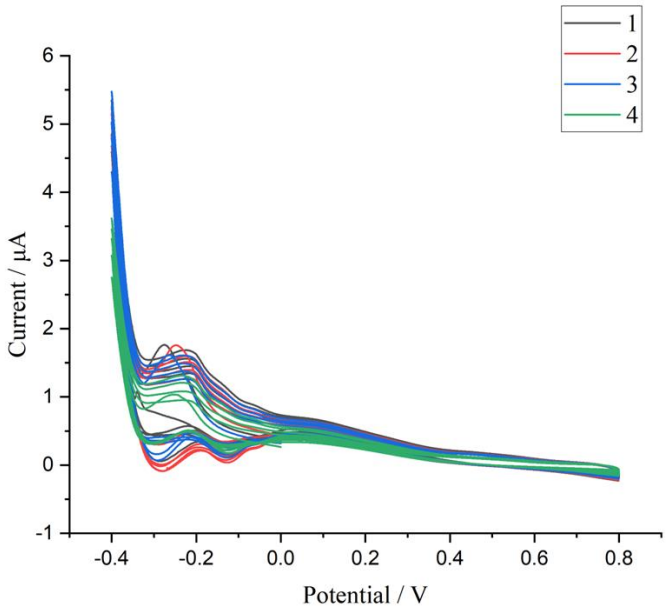

Figure 2.8 *Cyclic voltammogram for Pt-black deposition on four different electrodes*

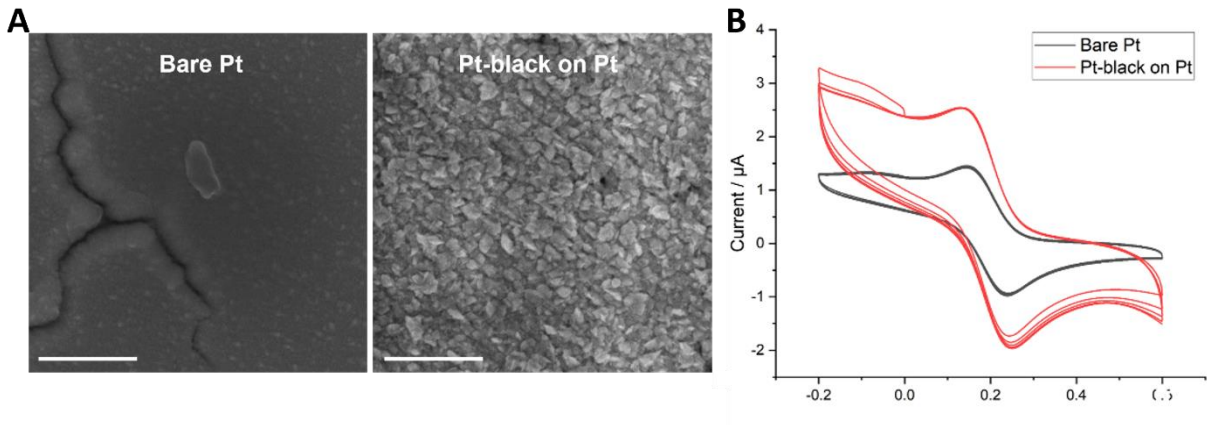

Figure 2.9 *A. Scanning Electron Microscopy (SEM) images for bare Pt and Pt-black electrodeposited on Pt, showing the nanostructures deposited through the Pt-black deposition (Scale bar = 1 µm). B. Cyclic voltammograms for the two probes using $K_3Fe(CN)_6$ as the redox couple.*

increase the active surface area for higher current response, electrochemical deposition of nanostructures, specifically Pt, was chosen. Because Pt is a very costly noble metal, electrodeposition provides a facile and cost-effective way to form nanostructures on the sensor surface [69, 70]. This method specifically lets Pt to be adhered to the electrode surface with no spare Pt being wasted, yielding the optimal output in a cost-effective manner. Also, surface modification via electrochemical deposition can be monitored during the process and the consistency throughout multiple probes can be validated by looking at the resulting cyclic voltammogram for the peak potentials and peak currents (Figure 2.8).

To validate the increase of surface area through electrodeposited Pt-black nanoparticles, scanning electron microscopy (SEM) and quantification of the surface area through electrochemical measurements were performed. Two surfaces, bare Pt and Pt-black deposited Pt were prepared and compared for this. As shown in Figure 2.9.A, when observed under the SEM, Pt-black nanostructures were observed for the samples after deposition, but for bare Pt, just a plain metal surface was observed. Thus, nanostructure formation via electrochemical deposition of Pt-black was confirmed through optical

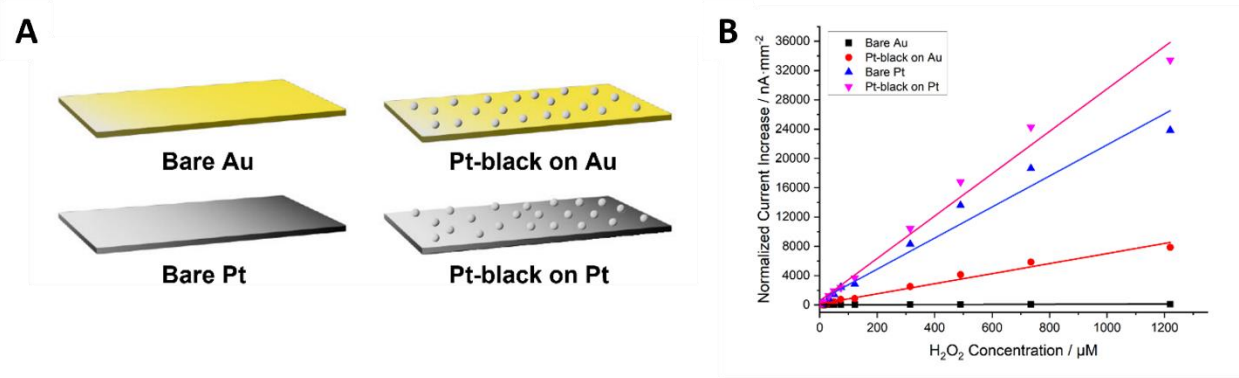

Figure 2.10 *A. Four different compositions of metals tested for oxidative properties towards H_2O_2. B. H_2O_2 sensitivity calibration curve for the four compositions (sensitivity: Pt-black on Pt > Bare Pt > Pt-black on Au > Bare Au).*

validation via SEM (Tescan GAIA3, Brno-Kohoutovice, Czech Republic). Then, to further validate the surface area enhancement, the active surface area of the samples was electrochemically quantified using Randles-Sevcik equation. Potassium ferricyanide ($K_3Fe(CN)_6$) was used as the redox couple and cyclic voltammetry was performed to retrieve the peak currents to derive the surface area. When the peak current from the cyclic voltammogram shown in Figure 2.9.B was substituted into the Randles-Sevcik equation, the calculated active surface area of Pt-black coated Pt was about 1.8 times higher than that of bare Pt probe (from 4207.07 μm^2 to 7567.33 μm^2). Thus, using both optical and electrochemical methods, SEM and Randles-Sevcik equation, it was validated that the electrodeposition of Pt-black nanostructures efficiently enhances the surface area of the electrodes that can possibly lead to increase in sensitivity.

Then, the surfaces' oxidative properties towards H_2O_2 were tested. H_2O_2 is the reporter molecule for the enzymatic reaction used for Glu and GABA and this gets oxidized by the polarized sensor surface, generating current (Figure 2.1). Thus, various combinations of materials (bare Au, bare Pt, Pt-black deposited Au, and Pt-black deposited Pt) were compared and tested to find the optimal metal layer to be used for the dual

Glu:GABA sensor (Figure 2.10.A). Au is a widely used metal for electrophysiological studies, such as electrocardiogram (ECG) and electroencephalogram (EEG) measurement, and Pt is known for its superior electrochemical activity during redox reactions compared to other noble metals [71]. Thus, these two metals with and without Pt-black surface modification were chosen to be compared for their oxidative performance towards H_2O_2. As expected, for both Au and Pt, Pt-black deposited surfaces showed higher sensitivity towards H_2O_2 when compared to the bare ones (Figure 2.10.B), showing the effect of increase in surface area through Pt-black nanostructures contributing to sensitivity enhancement. Further, even bare Pt showed higher responses than Pt-black deposited on Au confirming Pt's superior oxidation capabilities towards H_2O_2. Overall, Pt-black deposited on Pt showed the highest sensitivity, and so, this composition was selected as our sensing material for the experiments that follows.

2.4.2 *In vitro* Validation for Sensitivity and Selectivity

To validate the fabricated sensor for Glu and GABA detection, it was first calibrated *in vitro*. Self-referencing strategy was used on the microelectrode array probe, where there is another recording site close to the actual recording site that monitors any other signal except for the target molecule [72]. Briefly, the self-referencing site has the identical dimensions and composition as the sensing site but excluding the enzyme that reacts with the target neurotransmitter. By having a site with a blank enzymatic layer with similar thickness next to the sensing site, the self-referencing site receives the same ambient noise as the sensing site. Thus, for example, as shown in equation (3), while the Glu sensing (working) detects the current generated from Glu along with the faradaic and non-faradaic currents that are caused by other electroactive molecules that reaches the sensing surface,

the self-referencing site detects all the noises excluding the signal from Glu. These two signals can later be subtracted to enhance the signal-to-noise ratio (SNR), eliminating any signals that are generated from other molecules aside from the target.

$$i_{working} = i_{Glu} + (i_{F1} + i_{F2} + \cdots + i_{Fn}) + (i_{nonF1} + i_{nonF2} + \cdots + i_{nonFn})$$

$$i_{self-ref} = (i_{F1} + i_{F2} + \cdots + i_{Fn}) + (i_{nonF1} + i_{nonF2} + \cdots + i_{nonFn})$$

$$i_{Glu} = i_{working} - i_{self-ref} \qquad (3)$$

To find out our sensor's Glu sensitivity, the probes were immersed in 37°C 1X PBS with magnetic stirring while known concentrations of Glu ranging from 5 to 100 μM were dropped in the PBS sequentially. From the resulting current increase (Figure 2.11.A), the sensitivity for Glu was analyzed and the limit of detection was calculated by dividing the 3 times the standard deviation of the baseline by the least squares slope. As in Figure 2.12.A, our sensor showed a good linearity towards Glu with a sensitivity of 1.74 nA·mm^{-2}μM^{-1} (R^2=0.991) and a limit of detection (LOD) of 0.12 μM. GABA sensitivity was validated

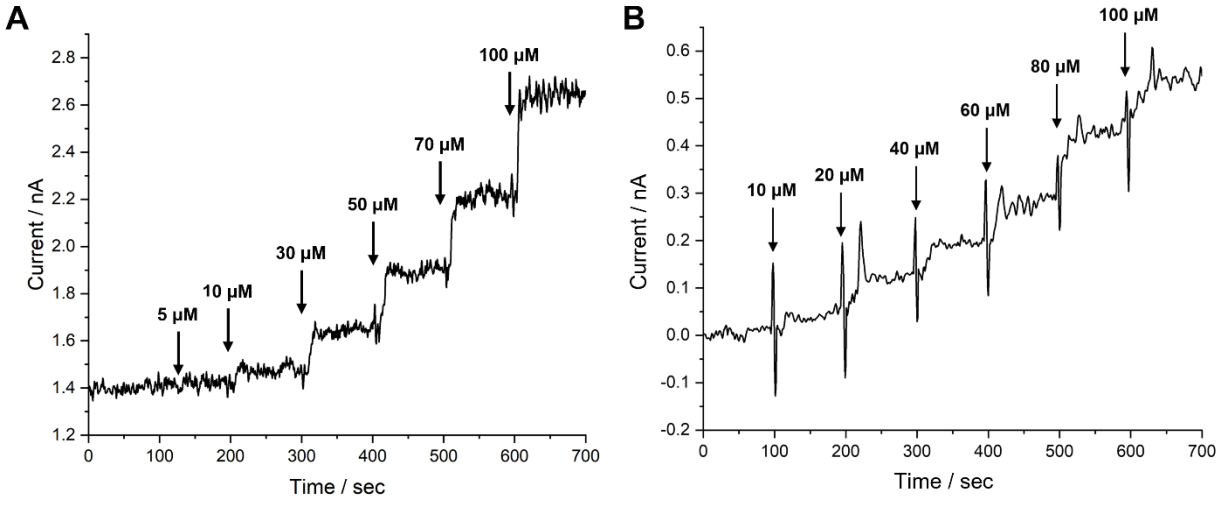

Figure 2.11 *Sensitivity test of the dual sensor probe for A. L-glutamate (5 to 100 μM) and B. GABA (10 to 100 μM).*

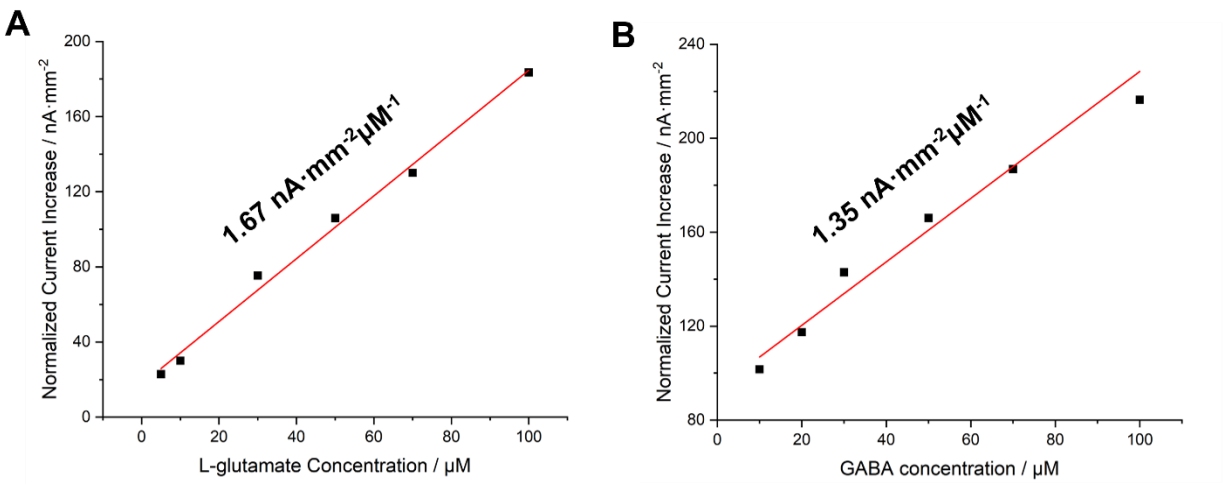

Figure 2.12 *Calibration curve with sensitivity for A. L-glutamate ranging from 5 to 100 μM and B. GABA ranging from 10 to 100 μM.*

similarly, where in this case, 1 mM α-ketoglutarate solution was used instead of 1X PBS due to the need of a precursor for the GABase reaction to occur. Known concentrations of GABA was added ranging from 10 to 100 μM (Figure 2.11.B) to the α-ketoglutarate solution and as in Figure 2.12.B, our sensor showed a good linearity with a sensitivity of 1.34 $nA{\cdot}mm^{-2}\mu M^{-1}$ (R^2=0.968) and a LOD of 0.04 μM, which is more sensitive than the previously reported sensors with bare Pt working electrode.

After validating its sensitivity, the sensors were subjected to a selectivity test for its specificity towards the target neurotransmitters. The experimental setup was similar to the sensitivity tests but interference molecules such as 250 μM AA and 2 μM AA were added along with Glu and GABA. As shown in Figures 2.13.A and 2.13.B, addition of the target neurotransmitters (20 μM Glu and 20 μM GABA) generated current only at the sensing and not at the self-referencing site, showing our sensor's specificity. When the interferent molecules were injected to the solution, there was no increase in current for both the sensing and the self-referencing sites showing that the mPD layer successfully repels them through size exclusion. Finally, when molecules that could cause ambient noise were

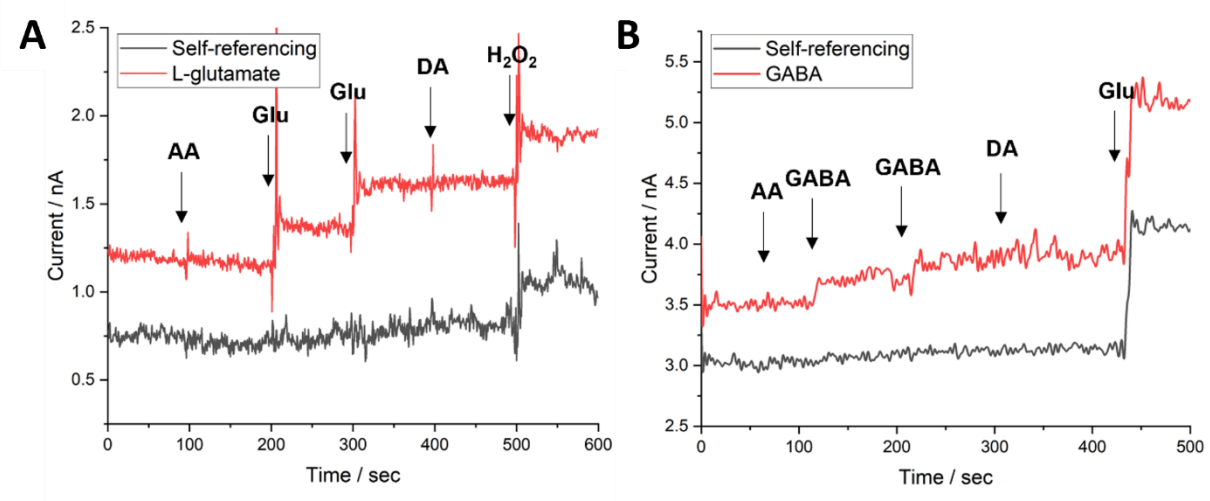

Figure 2.13 *Selectivity test for A. L-glutamate and B. GABA with addition of interferent molecules (ascorbic acid and dopamine). The sensing sites for L-glutamate and GABA only react to the target neurotransmitters while the self-referencing sites do not show any increase, showing the sensor's specificity. No significant current increase was observed for the interferent molecules (AA and DA), indicating the sensor's selectivity.*

introduced (9 μM H_2O_2 for Glu and Glu for GABA), signals were observed at both sites, which can later be subtracted from each other to increase the signal-to-noise ratio (SNR).

2.4.3 *Ex vivo* Validation

Further validation in *ex vivo* with neuronal cell culture was performed before implanting the probes *in vivo*. As shown in the cell culture timeline (Figure 2.14.A), the iPSCs were differentiated for 3 weeks into neural progenitor cells (NPCs), where the NPCs were further cultured for 2 more weeks to reach a stable status. Lastly, astrocytes were mixed with the NPCs and grown for 10 days to provide the adequate stimulation that they need to achieve the excitatory glutamatergic neurons. To confirm that the cells have been successfully differentiated into glutamatergic neurons, the cells were stained with DAPI, glial fibrillary acidic protein (GFAP), and β3T, which stains for cell survival, astrocytes and neurons respectively as shown in Figure 2.14.C. From this immunohistology, we were able

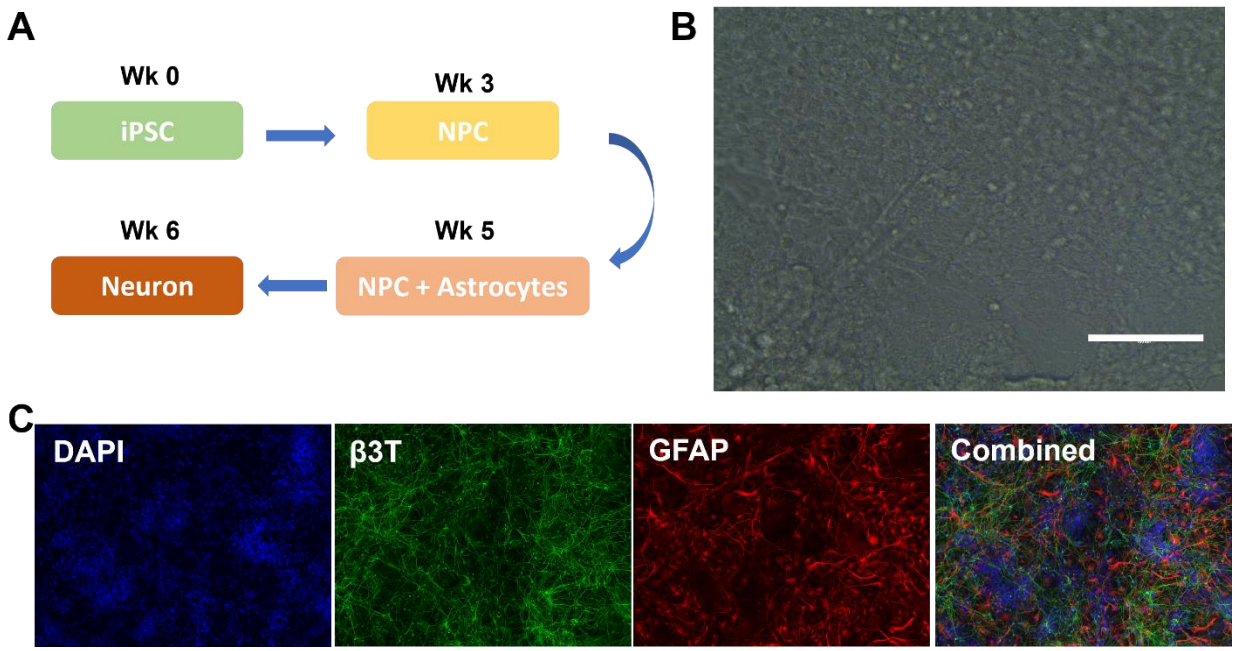

Figure 2.14 *A. Glutamatergic neuron culture process. B. Optical image of the differentiated glutamatergic neuron (Scale bar = 100 μm). C. Cell staining with DAPI, β3T, and GFAP for cell survival, astrocytes, and neurons, respectively.*

to confirm that the cells cultured were in fact the glutamatergic neurons that we tried to obtain.

Once the glutamatergic neurons were ready for measurement, the neurotransmitter sensors were tested for Glu detection. The cells were kept at 37°C and in aCSF to maintain their activity during measurement and 70 mM of KCl was added locally to the cells for stimulation after establishing a stable baseline. As in Figure 2.15, following KCl stimulation, there was a sharp increase in Glu signal within 10 seconds while no observable current change occurred at the self-referencing site, indicating that the sensor successfully detected Glu release from the glutamatergic neurons. Also, based on *in vitro* calibration performed right before the *ex vivo* testing, the current increase from the glutamatergic cells following the stimulation corresponded to 70 μM of Glu.

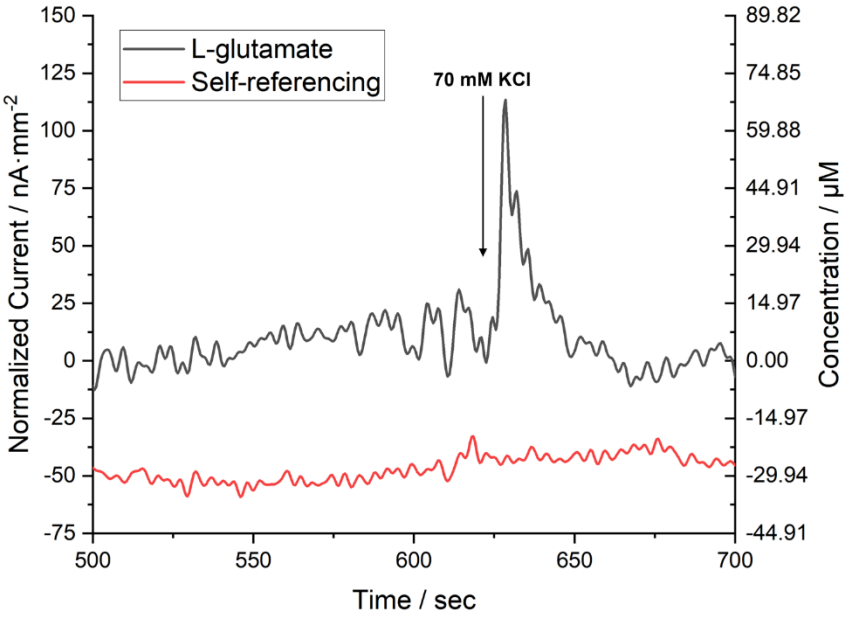

Figure 2.15 *Ex vivo recording. L-glutamate detection using the fabricated sensor showing the signals at L-glutamate sensing site and self-referencing site. The y axis on the right shows the L-glutamate concentration correlating to the current based on the calibration curve.*

2.4.4 *In vivo* Validation

After the sensors were validated *in vitro* and *ex vivo*, they were finally tested *in vivo* to investigate its performance for dual Glu:GABA sensing in animal models. Using a stereotaxic holder, the dual Glu:GABA sensor was inserted into cortical layer 4 of the rat's primary barrel cortex. The recording started after giving it around 30 minutes of stabilization period and with 70 mM KCl stimulation, current changes in both GABA and Glu were observed. As shown in Figure 2.16, sharp increases in current were noticed for both GABA and Glu after KCl stimulation, with GABA signal higher than that of Glu. Based on the design of the sensor, GABA sensing pad reacts to both GABA and Glu, while the Glu sensing pad only monitors the Glu level in the extracellular space. In other words, GABA sensing site records signals from both Glu and GABA while Glu sensing site records only Glu

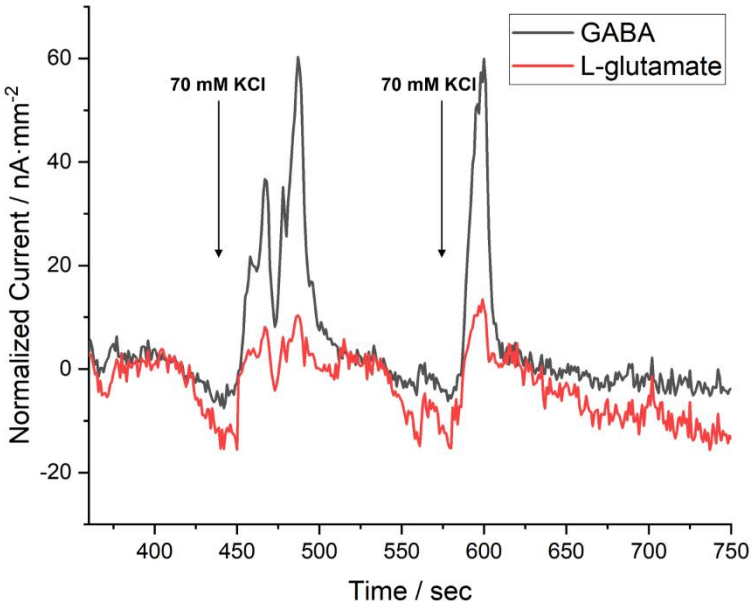

Figure 2.16 *In vivo recording. L-glutamate and GABA signals from 70 mM KCl stimulation in anesthetized rat's brain. While the L-glutamate sensing pad records the L-glutamate signal, since GABA sensing pad has both L-glutamate oxidase and GABase on the surface, it records signals from both L-glutamate and GABA. Thus, the signal from L-glutamate sensing pad needs to be subtracted from GABA sensing pad to retrieve the signal from GABA. The sensor showed similar level of current increase for both GABA and L-glutamate to the consecutive stimulation, which corresponds to 11.98 μM of L-glutamate and 29.63 μM of GABA.*

signal. Thus, when the signal from Glu sensing pad is subtracted from that of GABA sensing, amount of current change generated from GABA release can be calculated. Overall, from the two chemical stimulations, consistent increase in current was observed for both Glu and GABA, where these correlate to 11.98 μM of Glu and 29.63 μM of GABA based on the *in vitro* calibration performed right before the *in vivo* measurement.

2.4.5 Additional Features for the Sensor Performance

Sensitivity and selectivity are among the most important features when developing a sensor platform, but considering the fabrication process and the specific purpose for detecting neurotransmitters *in vivo* for a long period of time, there were other aspects that needed to be thought out regarding the dual Glu:GABA sensor. First, the longevity of the

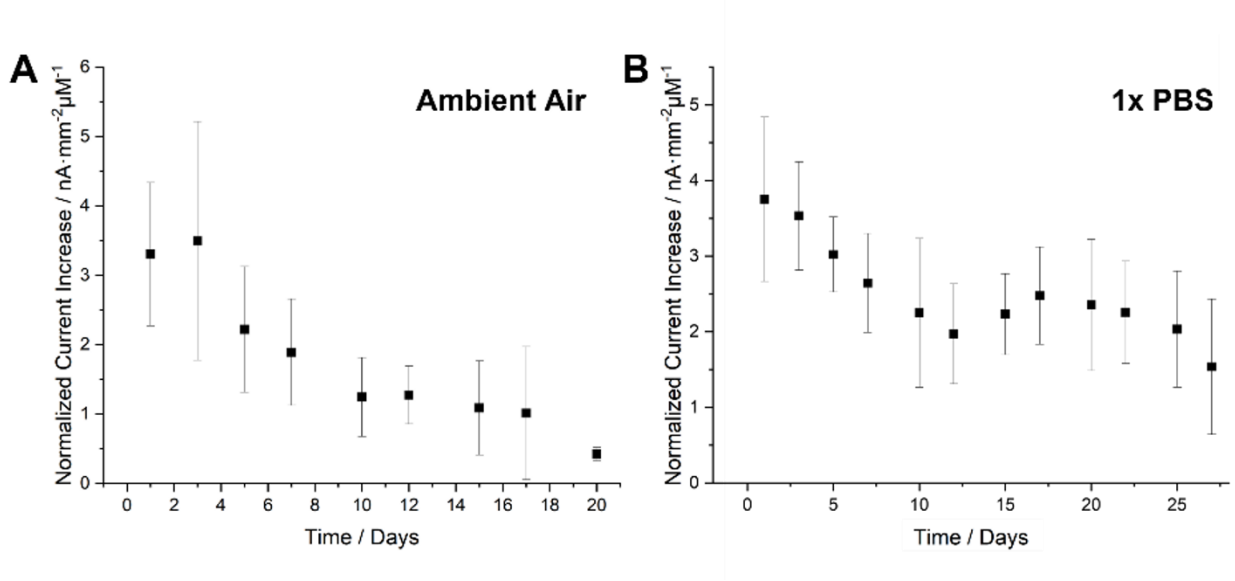

Figure 2.17 Longevity test. *The longevity of the enzymatic neurotransmitter sensor when kept at* ***A.*** *ambient air, and in* ***B.*** *1X PBS, showing sensors in PBS shows higher longevity along with slower decrease in enzyme activity. (n=3)*

sensor was investigated to better understand the sensor's lifetime with the optimal period that the sensor can be used for. Since the dual Glu:GABA sensor utilizes enzymes (GOx and GABase), the sensor's lifetime is highly dependent on the lifetime of the enzymes applied on the sensor which is relatively short [73-75]. Thus, the longevity of the sensors was evaluated to see how long they can last as well as exploring the optimal storage method. Two storage conditions were compared to find the optimal method to keep the neurotransmitter sensors active for longer time. The sensors were divided into two groups, one was stored in ambient air and the other in 1X PBS. They were tested every two days for its response to 20 µM Glu and the resulting plots are shown in Figures 2.17.A and 2.17.B. For both conditions, the sensors were able to detect Glu for more than 3 weeks. However, the sensitivity of the sensors kept in ambient air decreased faster than that of PBS, indicating that the sensors kept in PBS maintained its activity better. The reason behind this can be assumed from the fact that keeping the sensors in 1X PBS helps the enzymes maintain their physiological properties, while keeping them in ambient air in room

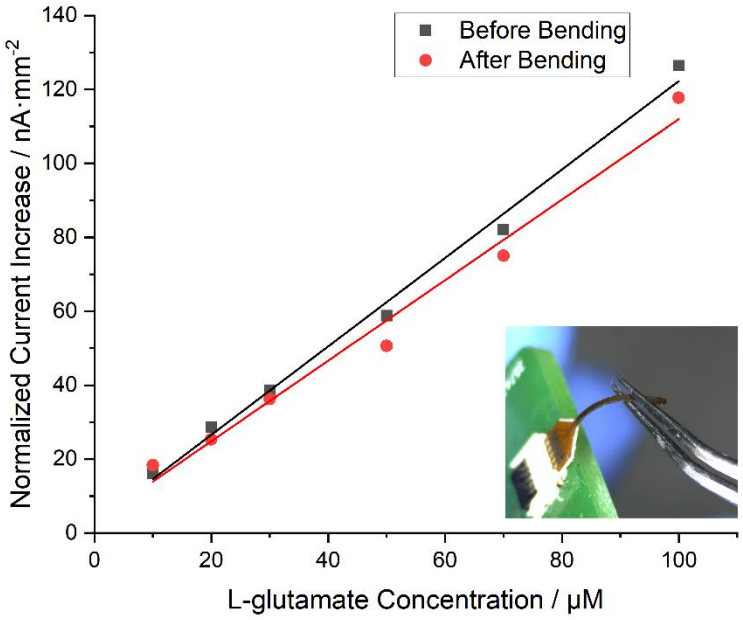

Figure 2.18 *Calibration curve for L-glutamate sensitivity before and after bending at 70 degrees for 100 times. Inset demonstrates the flexibility of the developed dual L-glutamate:GABA sensor probe.*

temperature can dehydrate the enzymes. Also, for the same reason, the sensors in PBS showed longer longevity for about a month when the ones in ambient air lost their activity after 20 days. This result shows that keeping the sensors in PBS is a more effective storage method and helps speculate that once implanted *in vivo*, the sensors would be good for about a few weeks.

Another aspect investigated was the flexibility of the sensor. While there are other dual Glu:GABA sensors the have been reported, they were all fabricated on the ceramic substrate. Ceramic can provide rigidity and easy handling during the fabrication process, but it is also fragile during implantation. Our experiences with *in vivo* studies showed that sensors made of rigid silicon or ceramic are very prone to break. This is not only very costly but also extremely inconvenient as the entire experiment can be ruined by such an incident. Thus, we chose flexible polyimide with an appropriate thickness (125 µm) as our

substrate, where it does not break but still penetrates the brain with its flexibility. The inset of Figure 2.18 demonstrates how flexible the developed sensor is and to check if the sensor still maintains its performance after being bent continuously, the neurotransmitter sensor has been subjected to a sensitivity test before and after bending at 70° for 100 times. As seen in Figure 2.18, our sensor maintained 93% of its sensitivity after rigorous bending, indicating that the proposed sensor can withhold the distortion during implantation and animal movements during the measurements with consistent performance.

2.5 Conclusion and Future Works

In this study, a flexible dual Glu:GABA sensor with high sensitivity has been demonstrated for detecting neurotransmitters in the central nervous system for neurological studies. Using flexible polyimide as a substrate, the biosensor is easy to handle during implantation and measurements while maintaining its sensitivity. Further, Pt-black nanostructures were electrodeposited onto the sensing surface to increase the active surface area that led to higher sensitivity towards Glu and GABA. The mPD coating along with self-referencing technique allowed target specific sensing and higher SNR. These advancements of the sensor were validated thoroughly in various settings, such as *in vitro* lab environments, *ex vivo* in glutamatergic neuronal cell cultures, and *in vivo* in the anesthetized rat. Additionally, we have investigated an optimal storage method to enhance the sensor's longevity.

Overall, real-time monitoring of neurotransmitter level changes *in vivo* is highly in demand for studying the mechanisms behind neurological disorders. Not only does our dual Glu:GABA sensor can easily be used for monitoring the neuronal differentiation or any

cell culture platform for neuroscience due to its flexibility, we specifically plan to apply our sensor to look at the mechanism of Glu:GABA imbalance related to early life sleep disruption (ELSD) models with relevance to E:I imbalance reported in ASD. Based on the recent findings regarding specific brain pathology associated with ASD, such as overgrowth of dendritic spines that can lead to increased glutamatergic excitation and reduced numbers of GABAergic interneurons [76-78], there is a possibility of E:I imbalance in development of ASD where further investigation is needed. The dual Glu:GABA sensor presented in this study can provide a tool for this purpose of detecting neurotransmitters *in vivo* with minimal brain damage with high sensitivity and this will bring the field a step closer to investigating the cause for neurological disorders.

2.6 Acknowledgements

The authors would like to acknowledge the financial support from the NSF CAREER Award #1917105 to H.C. and the NSF NCS Award #1926818 to H.C. and M.M.L.

CHATPER 3: Polarized IrOx as Reference Electrode Material for Biocompatible L-glutamate Sensor

Sung Sik Chu[1], Xing Xia[2], Hung Cao[1,2,3,4]

Affiliation

[1]Department of Biomedical Engineering, University of California Irvine, CA, 92697, USA

[2]Department of Electrical Engineering and Computer Sciences, University of California Irvine, 92697, CA, USA

[3]Center for Neural Circuit Mapping, University of California Irvine, CA, 92697, USA

[4]Department of Computer Science, University of California Irvine, CA, 92697, USA

3.1 Abstract

Long-term monitoring of neurotransmitter levels *in vivo* is an area of interest to investigate the mechanism behind neurological disorders. Electrochemical sensors are currently being explored for this purpose with the advantages of miniaturization and fast response time. However, although many reports have been made in terms of its performance, the biocompatibility of the electrochemical sensors are not as thoroughly addressed. Currently, for electrochemical *in vivo* neurotransmitter recordings, Ag/AgCl wire pseudo-reference electrode is being widely used. Despite its advantage in stability, AgCl has been reported for its biofouling properties and this external electrode requires additional insertion area to be created in the brain, causing bigger brain damage. Therefore, in this work, a polarized IrOx pseudo-reference integrated L-glutamate sensor is developed for long-term neurotransmitter measurements. On-probe IrOx thin film has been electrochemically deposited and confirmed with EDS and optical methods. Then its characteristics such as pH dependence, stability and biocompatibility have been tested. In addition, polarization of IrOx is introduced to further enhance its stability. Overall, the polarized IrOx on-probe L-glutamate sensor demonstrated highly enhances the biocompatibility of the electrochemical sensing platform. Thus, this sensor should aid investigation of mechanisms behind various neurological disorders through long-term monitoring of neurotransmitters.

Keywords: L-glutamate, electrochemical sensor, IrOx thin film, polarization, biocompatbility

3.2 Introduction

Neurotransmitters are chemical substances that are released from the end of a nerve fiber which results in either excitation or inhibition of the post-synaptic neuron. There are vast number of neurotransmitters present in mammals and these are assumed to play a vital role in neurological disorders [79]. However, due to the lack of technology to track the neurotransmitter levels real-time *in vivo*, a lot of neuroscientists and engineers are in the process of finding an adequate method for long-term, real-time neurotransmitter measurement [80]. While various techniques are being explored, electrochemical sensors are gaining attention due to their fast response time and superior spatiotemporal resolution [81]. In this regard, multiple electrochemical neurotransmitter sensors have been reported for detecting L-glutamate (Glu), GABA (γ-aminobutyric acid), dopamine, serotonin, glucose, etc. [82] Furthermore, the field has been transitioning from targeting single neurotransmitters to simultaneous neurotransmitter sensing to look more in depth at how multiple neurotransmitters affect neurological disorders [83-85]. However, while there has been an extensive breakthrough in terms of sensitivity and its sensing mechanism, not much has been reported for the neurotransmitter sensor's biocompatibility for long-term measurements.

Most of the electrochemical neurotransmitter sensors that have been reported so far utilized an external pseudo-reference electrode (RE) such as silver chloride (AgCl) coated silver (Ag) wire for *in vivo* measurement. Although Ag/AgCl wire pseudo-RE is known for its stability, it is not a biocompatible material [86-88] and this additional electrode aside from the sensing electrode (working electrode) requires another implant

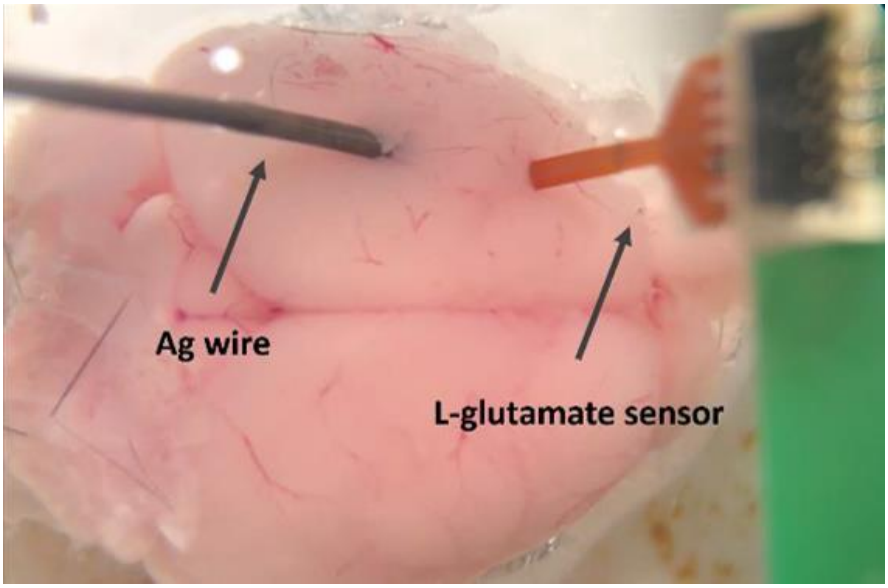

Figure 3.1 *Demonstration of in vivo brain electrochemical measurement with Ag/AgCl pseudo-RE*

site to be drilled onto the skull for *in vivo* neurotransmitter recordings [89], damaging more area of the brain (Figure 3.1). Additionally, usage of Ag/AgCl wire as a pseudo-RE was feasible for most of the *in vivo* experiments because many of them were performed with anesthetized animals, where there's no movement and are not long-term measurements. However, to record neurotransmitter signals from freely behaving animals, Ag/AgCl wire pseudo-RE would not be the best choice due to concerns such as complication in multiple electrode implantation and possibility of electrode movement leading to noise in signal. Therefore, integrating the RE onto the sensor itself using a better biocompatible material would be the optimal choice to alleviate the stress for the subject while performing long-term neurotransmitter measurement.

Currently, iridium oxide (IrOx) thin film is widely being investigated in electrochemical field for their use in pH measurement [90-92]. After being first reported by Yamanaka et al. in 1989 [93], iridium-based films have been of interest for various applications. Specifically, its intrinsic properties including linear sensing performance for

measurements of wide range of pH (pH dependence), minimal interference from ions, and the ability to operate in wide range of temperatures without additional treatment makes them an attractive material to be used for pH sensing [94]. There are multiple ways to obtain IrOx thin films such as thermal oxidation, sputtering, sol-gel deposition, anodic electrodeposition, etc [95, 96]. And IrOx films resulting from different fabrication processes show different performance in terms of sensitivity and stability. However, the characteristic of interest for IrOx thin film in this chapter is their biocompatibility. For pH measurements, this is often looked down on since most of the measurements are done with either sample *in vitro* or temporarily *in vivo*. But for long-term measurements *in vivo*, the biocompatibility of the material is one of the most important properties of a material that needs to be considered. IrOx has been reported as a material that shows greater biocompatibility when compared to other metals or metal composites that are commonly used as a RE for *in vivo* recordings. Despite its pH dependence, as mentioned, the physiological pH range of brain is relatively small between 7.15 to 7.4 [97], making it a potential material as a stable and biocompatible RE. Thus, in this paper, we validate IrOx's performance as an on-probe pseudo-RE for Glu sensor and further suggest a method to enhance its stability by polarizing the IrOx layer. By doing so, we aim to develop a biocompatible, RE integrated Glu sensor to minimize any inflammatory response for longer stability *in vivo* for long-term neurotransmitter measurements.

3.3 Materials and Methods

3.3.1 Materials

Phosphate buffered saline (10X PBS), glutaraldehyde, and 30% hydrogen peroxide (H_2O_2) were purchased from Thermo Fisher Scientific (Waltham, MA). 97+% L-glutamic acid monopotassium salt monohydrate, 99% dopamine hydrochloride (DA), and 97% bovine serum albumin (BSA) were purchased from Alfa Aesar (Haverhill, MA). L-ascorbic acid (AA), and 99% m-phenylenediamine dihydrochloride (mPD) were purchased from Acros Organics (Fair Lawn, NJ) and glutamate oxidase (GOx) from US Biological Life Science (Swampscott, MA). Ag plating solution (Potassium cyaniade and silver cyanide) was purchased from Transene (Danvers, MA) and oxalic acid dihydrate, potassium carbonate from Sigma Aldrich (St. Louis, MO).

3.3.2 Microelectrode Array Design and Fabrication

The microelectrodes were first fabricated in the clean room using photolithography. The substrate, flexible polyimide film, was thoroughly cleaned with acetone, isopropyl alcohol (IPA) and deionized water (DI water) for organic particle removal. After drying the films with nitrogen gas, negative resist (NR9) was spin-coated on top. To pattern the electrode layer, ultraviolet (UV) light was exposed to the photoresist followed by baking the substrate. Then the NR9 on the film was developed to define the traces and pads and onto the NR9 patterned polyimide film, 20 nm of chromium (Cr) and 200 nm of platinum (Pt) were deposited using electron beam evaporator with 7.3 kV of voltage, 160 mA of current, and 0.8 – 1.2 Å/sec of deposition rate. Here, Cr was deposited prior to Pt for better adhesion of Pt to the polyimide surface. Then using a lift-off process, the metal deposited substrates were ultrasonicated in acetone and IPA for 5 minutes each to leave the metal

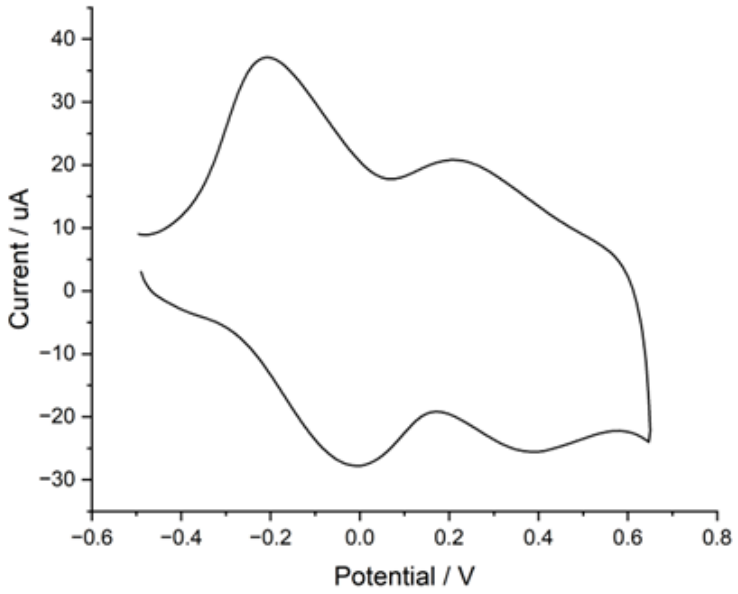

Figure 3.2 *Cyclic voltammogram for IrOx deposition process*

traces (Pt) only at the regions with direct contact. As the last layer of the electrode, an SU-8 barrier layer was formed by spin-coating SU-8 2000. This photoresist was further baked and developed to obtain the initial form of the sensor. Finally, the batch of probes within 4-inch circular polyimide consisting around 90 probes were then sent to LASEA Inc. (El Cajon, CA) for laser cutting.

3.3.3 Reference Electrode Surface Modification

To compare the performance of IrOx RE to other REs that are used for pseudo-RE purposes, four different types of REs were prepared. Commercially available glass Ag/AgCl reference electrode was purchased from BASi (West Lafayette, IN) and Ag/AgCl wire, AgCl coated, and IrOx coated pseudo-REs were fabricated in lab. To coat the IrOx onto the Pt probe, oxalate-$IrCl_4$ plating solution (Yamanaka solution) was first prepared with a composition of 0.14% $IrCl_4$, 99.36% water, and 50% $C_2H_6O_2$. Then using potassium carbonate (K_2CO_3), the pH of the solution was adjusted to 10.5 and kept at room temperature for 3 days before use. For the actual coating via electrodeposition, the Pt

probe was immersed into the prepared Yamanaka solution and potential ranging from -0.5 to +0.65 V v.s. a glass Ag/AgCl RE was cycled with a scan rate of 0.1 V/s for 200 cycles. The electrodeposition process for IrOx was monitored with the resulting cyclic voltammogram and four peaks (two for oxidation and two for reduction) were observed for successful coating (Figure. 3.2). For the fabrication of Ag/AgCl wire, commercially available silver wire with a diameter of 0.5 mm was immersed in 1M KCl. Then an anodic current of 500 μA v.s. a Pt counter electrode was applied for 5 minutes for chlorination of the silver wire. Lastly, to fabricate the AgCl coated pseudo-RE, surface modification of Pt probe was performed to first create a silver layer on top using Transene Ag plating solution. Onto the immersed probe, constant cathodic current of 18 μA v.s. a Pt counter electrode was applied for 60 sec and rinsed with water. Following this surface modification, a similar chlorination step in 1M KCl took place by applying constant anodic current to the Ag coated electrode as we did for Ag/AgCl wire fabrication. However, the current and deposition time had to be adjusted according to the size difference between a wire and the sensing pad on the probe. Thus, constant anodic current of 0.5 μA v.s. a Pt counter electrode was applied for 600 sec to achieve the final AgCl coated probe for pseudo-RE. After all the fabrication processes, the REs were rinsed with DI water and set aside for further use.

3.3.4 Surface Modification for L-glutamate Detection

As for the working electrode (WE) of the sensor, for the sensor's specificity towards Glu, L-glutamate oxidase (GOx) was deposited on the sensing pads. Since Glu is not electroactive, a mediator is required to convert this non-electroactive molecule into an electroactive molecule. In this case, the mediator is GOx and the resulting electroactive molecule is H_2O_2, which gets oxidized at the WE surface. So, to deposit the enzymes, an

enzymatic mixture was made by initially dissolving 10 mg of BSA in 985 µl of DI water. After thoroughly dissolving the BSA with pipetting, 5 µl of glutaraldehyde was added as a crosslinking agent. The mixture was manually inverted 5 times and left at room temperature for 5 min for BSA to bind to glutaraldehyde. Meanwhile, GOx aliquoted (1U/1µl) and stored in -80°C were brought out to room temperature for thawing. Then the enzymes were mixed with the BSA solution to make 5 µl of the enzymatic solution, where the amine groups of the GOx binds to the other arm of the glutaraldehyde making a BSA-glutaraldehyde-GOx complex. As for the deposition, the probes were placed under a stereotaxic microscope and GOx solution was drop casted onto the pads designated as WE (approximately 0.05 µl/drop) with a Hamilton's syringe. A total of 3 applications were made to create the enzyme layer and one minute interval was given between each application. Once all the applications were complete, the enzyme-deposited probes were kept at 4°C for at least 2 days for stabilization.

Additionally, for the sensor's selectivity, an exclusion layer of mPD was electrodeposited. When mPD is electropolymerized, it forms a mesh structure that can block the interferent molecules via size exclusion. In the brain, where numerous neurotransmitters are present, molecules such as ascorbic acid (AA) or dopamine (DA) can cause noises that can interfere with the target neurotransmitter signals making them interferent molecules. Electrodeposited mPD exclusion layer is known to effectively repel these molecules, so it was adapted for this study as well. To make the mPD solution, 0.05 M PBS was purged with nitrogen gas for 20 min for deoxygenation and then mPD was evenly mixed into the deoxygenated PBS to create 5 mM of mPD solution. Once the enzyme deposited probes were immersed in the mPD solution, a potential was cycled between +0.2

to +0.8 V v.s. a glass Ag/AgCl RE for 15 min. When completed, the probes were rinsed with DI water and kept at 4°C for at least 24 hours before use.

3.3.5 IrOx polarization

Polarization of IrOx surface has been performed to stabilize the IrOx pseudo-RE for noise reduction. When in electrochemical measurements, the stability of the signal is highly dependent on the RE. In other words, as the stability of the RE increases, the stability of the resulting signal increases as well. In this regard, one of the methods of increasing the RE's stability is to simply increase the size of the RE. This relationship has been well established where higher stability can be achieved by using a bigger RE. However, for long-term continuous measurements *in vivo*, there are limitations in size that need to be thought of for minimal damage to the brain. In the engineering perspective, using a big RE for higher stability is favored but in the clinical perspective, smaller size electrodes are in favor for minimal brain damage. Also, bigger electrodes have a higher chance of penetrating the blood vessels in the brain, where the blood can interfere with the signals. Therefore, there is a need for small RE with good stability in the field of *in vivo* brain electrochemical measurement.

To address this, we tried polarizing the IrOx pseudo-RE to increase its stability. First to find out the optimal potential for polarization of our IrOx coated electrode, several polarizing potentials were tested. Once the IrOx pseudo-RE electrodes were ready, the probes were immersed in a 1X PBS solution, and a constant potential of interest were applied v.s. a glass Ag/AgCl RE for 1 min using chronoamperometry. Right after polarization, the IrOx pseudo-RE was kept in the same solution of 1X PBS and was tested for open circuit potential (OCP) to see its stability. These two steps were repeated with

several potentials to find out the polarization potential with least amount of drift in the OCP and that potential was chosen as the optimal potential used in further experiments.

3.3.6 Characterization and Calibration

Once the probes were fully prepared, they were subjected to performance validation using a multichannel potentiostat from Pinnacle Technology Inc. (8102-N, Lawrence, KS). For the basic setup of the experiment, a beaker containing 1X PBS was placed on top of a hot place set at 37°C along with constant magnetic stirring. Then the probes were lowered into the PBS solution to immerse the tip, where the sensing pads are located, and constant potential of +0.7V was applied against various REs being tested. After few minutes of

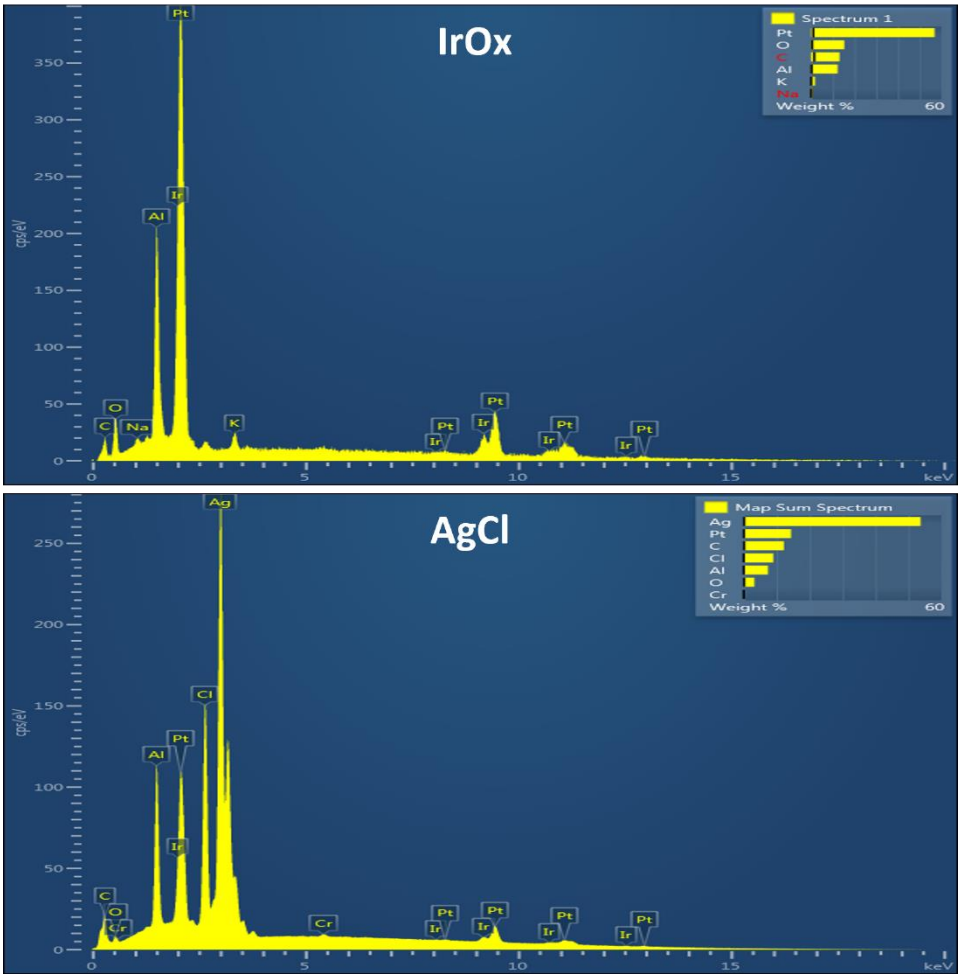

Figure 3.3 *EDS analysis for IrOx coated pseudo-RE and AgCl coated pseudo-RE*

stabilization period, known concentrations of Glu were added to the solution and the resulting amperometric curve was used for sensitivity and baseline noise analysis.

3.4 Results and Discussion

3.4.1 Material Optimization for Pseudo-Reference Electrode

In this study, four different REs (glass Ag/AgCl, AgCl wire, AgCl coated pad, IrOx coated pad) were used to test and compare its sensitivity and stability. While glass Ag/AgCl RE was commercially available and AgCl wire was fabricated following previously reported methods, the AgCl coated and IrOx coated pads first needed to be validated to check successful deposition. To do that, energy dispersive X-ray spectroscopy (EDS) was used to look at the elemental composition of the modified surfaces that have been electrodeposited with AgCl and IrOx. Once the specific pads of the probe were electrochemically deposited with either AgCl or IrOx, the probes were coated with 5nm of Ir for conductivity and were placed in a Tescan SEM chamber (GAIA 3, Brno, Czechia) for EDS analysis. As shown in Figure 3.3, when EDS was performed on both surfaces, a peak for Ag and Cl were observed on the AgCl coated surface while such peaks were not present for IrOx coated surface. Also, while Ir peaks are observed in both surfaces, the Ir peak for IrOx coated surface is much

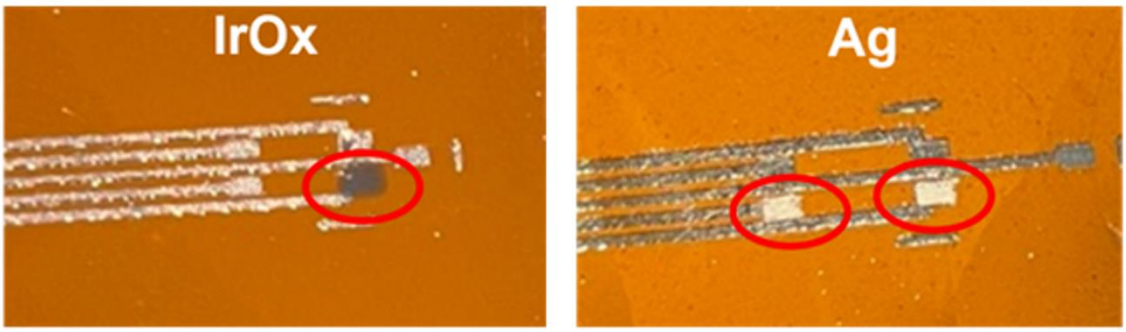

Figure 3.4 *Optical image of IrOx coated electrode and Ag coated electrode*

higher than that of AgCl coated surface distinguishing the electrodeposited IrOx from the sputtered Ir coating for SEM/EDS purposes. Other elements that showed up in the EDS analysis can be explained by the Pt metal layer of the basic form of the probe, Ir coating for conductivity, and composition of polyimide substrate. Additionally, the AgCl and IrOx coating showed optical differences under the optical microscope. The change in color was easily noticeable where bare Pt shows a silver color whilst IrOX coated surface demonstrates a purple color. For AgCl deposition, Ag was electrochemically deposited on Pt electrode first and was further chloridized. In this case as well, the change in color when Ag was deposited was clearly observable as shown in Figure 3.4. Thus, through both optical microscope and EDS, the electrodeposition of AgCl and IrOx have been validated.

3.4.2 IrOx Surface Characterization

Once the electrodeposition of AgCl and IrOx have been validated, the IrOx surfaces were subjected to polarization. But before that, the pH dependency of IrOx film was tested first by looking at its response to different levels of pH. Here, commercially available pH

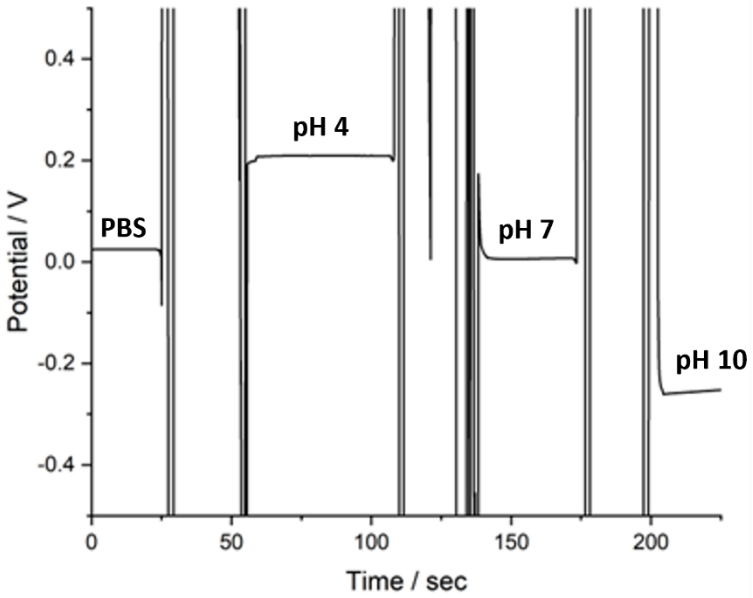

Figure 3.5 *pH dependent potential change of IrOx coated pseudo-RE.*

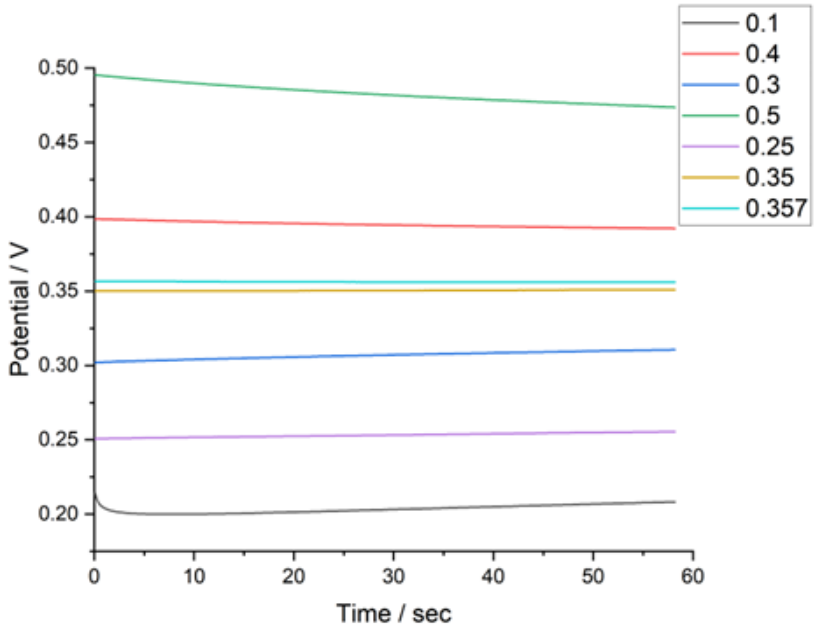

Figure 3.6 *OCP for IrOx pseudo-REs polarized with varying potentials.*

solutions of pH 4, 7, and 10 were prepared and the IrOx pseudo-RE was immersed into the solution sequentially in the order of 1X PBS, pH 4, pH 7, and pH 10. The pseudo-RE was rinsed in DI water in between when switching from one solution to the other and an OCP was ran v.s. a Ag/AgCl glass RE. For the results, as reported from other groups, IrOx coated electrode showed good pH dependency with stable potential for pH 4, 7, and 10 (Figure 3.5).

Then the drift of IrOx coated electrodes in different polarization potentials were compared to find the optimal potential for stabilization. As explained in the methods, the IrOx pseudo-REs were polarized in 1X PBS solution using various potentials ranging from 0.1 to 0.5 V, and OCP recordings were immediately followed to observe the drift in potential. As shown in Figure 3.6, when the polarizing potential was too extreme, such as 0.1 or 0.5 V, the potential drifted a lot within a short period of time. But the trend observed with extreme potentials was that they all drifted towards a certain potential in the middle.

Based on this information, we narrowed down the polarizing potential accordingly. As the polarizing potential narrowed down, less drift was observed and finally, when a polarizing potential of 0.357 V was used, the OCP signal was very stable. Therefore, polarizing potential of 0.357 V was identified as the optimal parameter.

3.4.3 IrOx Surface Characterization for Biocompatibility and Stability

The REs commonly used for neurotransmitter detection *in vivo* are AgCl coated silver wire pseudo-RE. However, there have been some concerns on the biocompatibility of AgCl, stating that it can cause inflammatory response *in vivo*. Also, implanting a whole another RE aside from the biosensor itself can damage more areas of the brain. Therefore, a single electrode that consists of both the working electrodes and RE with higher biocompatibility would be better for long-term measurements *in vivo*. IrOx is one of the promising materials to be used as a RE material since despite its pH dependence, the pH in the extracellular environment doesn't change much. In this regard, the performance of IrOx as a pseudo-RE material has been tested by checking its stability and comparing it with other REs that are available.

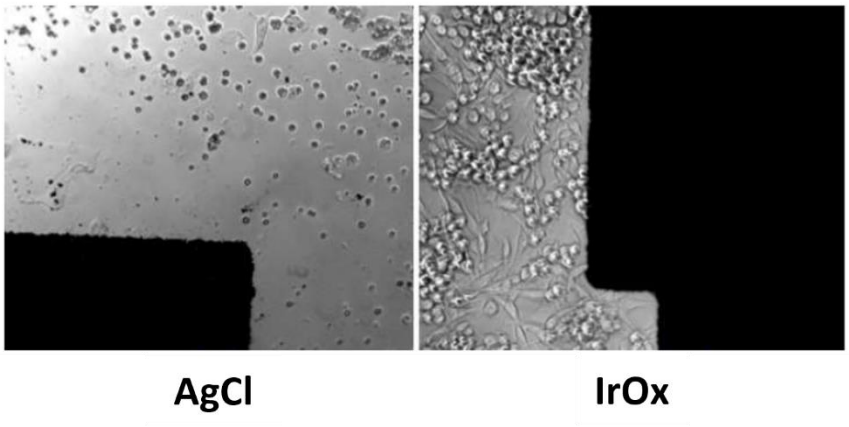

Figure 3.7 *Cell viability comparison between Ag/AgCl and IrOx for biocompatibility. The experiment was performed with an available line in the lab, PNT1-A cells.*

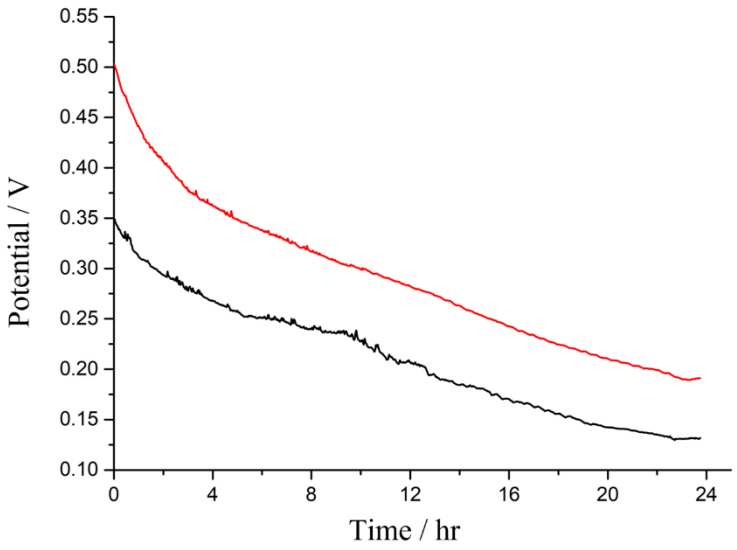

Figure 3.8 *Open circuit potential comparison between glass Ag/AgCl (red) reference electrode and IrOx pseudo-reference electrode(black).*

First, the biocompatibility of IrOx was tested using cell cultures and compared with AgCl, a pseudo-RE material reported as less biocompatible. On two different surfaces, IrOx and AgCl, PNT1-A cells were seeded and observed under a microscope after 3 days. As shown in Figure 3.7, while cells were not able to attach to the AgCl surface, cells on IrOx successfully adhered to the electrode validating IrOx's superior biocompatibility compared to AgCl in *ex vivo* settings. Next, to check the IrOx's stability as a pseudo-RE material, it was subjected to an OCP test against a glass Ag/AgCl RE for 24 hours. As shown in Figure 3.8, IrOx pseudo-RE showed relatively stable potential in respect to commercial glass Ag/AgCl RE for the time tested. This result indicates IrOx's capability of being used as a stable pseudo-RE for *in vivo* neurotransmitter sensors.

3.4.4 IrOx Polarization and Sensor Characterization

After confirming the biocompatibility and stability of IrOx, polarization's effect on IrOx surface has been tested. As mentioned above, IrOx pseudo-RE has been polarized with a constant potential of 0.357 V for 1 min to further enhance its stability. While IrOx thin

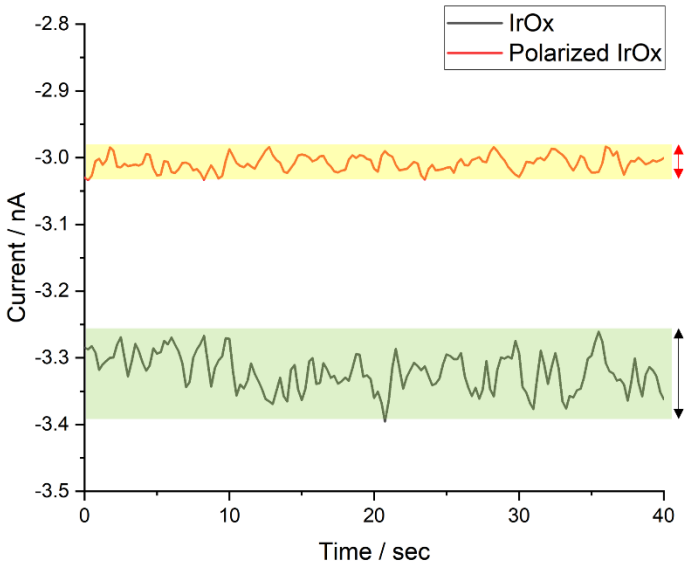

Figure 3.9 *Baseline stability comparison for polarized IrOx and untreated IrOx*

films show stability and greater biocompatibility compared to AgCl pseudo-REs, there are long-term drifting issues that limits its application [98]. To address this issue, Caroll et al. reported that by providing a constant potential to the IrOx film, it is possible to standardize the absolute potential response for individual electrodes in an array for extended period of time [99]. Furthermore, Olthuis et al. showed that different oxidation states result in varying drifting potentials [100]. Based on this information, we have hypothesized that constant voltage treatment to the IrOx thin film will alter its oxidation states possibly resulting in greater stability. To test this hypothesis, the baseline stability of IrOx thin film after polarization was tested against an untreated IrOx electrode. With the two electrodes immersed in 1X PBS, OCP was ran and as shown in Figure 3.9, the IrOx electrode after polarization resulted in lower baseline noise (fluctuation) compared to that of the IrOx without polarization. This shows that polarization helps enhance the baseline stability of IrOx.

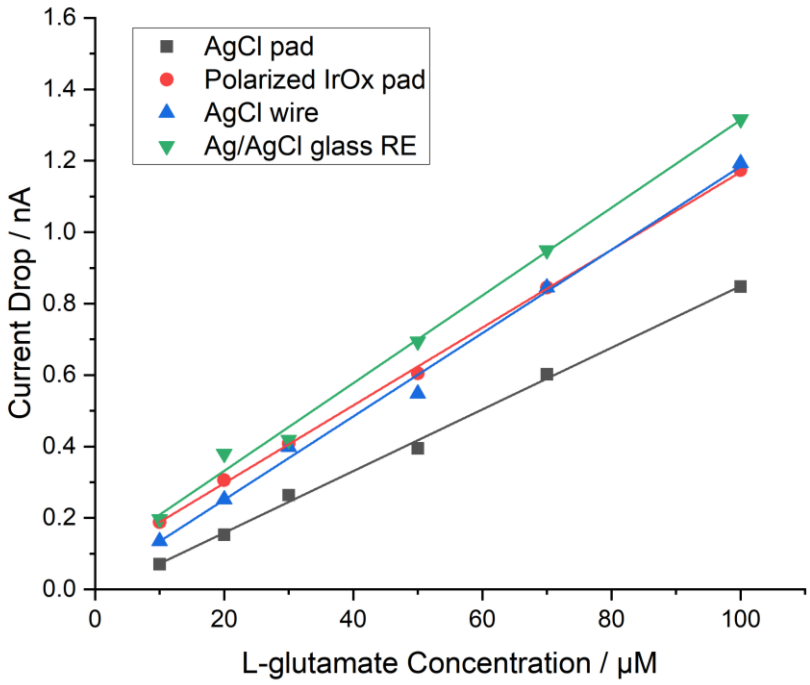

Figure 3.10 *The sensitivity plot for L-glutamate against 4 different reference electrode materials (Ag/AgCl bulky RE > AgCl wire ≈ IrOx pad > AgCl pad).*

Finally, the actual performance of polarized IrOx as a pseudo-RE for neurotransmitter detection was tested by comparing it with other RE materials. A total of 4 REs were compared, glass Ag/AgCl RE, AgCl coated Ag wire, AgCl coated Pt probe, and polarized IrOx probe. Then Glu sensitivity test was performed with 4 different materials as shown in Figure 3.10. As expected, the glass Ag/AgCl RE showed the highest sensitivity due to its high stability, while AgCl coated pad showed the lowest. As for the others, polarized IrOx pad and Ag/AgCl wire showed similar performance towards neurotransmitter sensing. This shows promising information that polarized IrOx can be a great substitute with similar sensing performance as Ag/AgCl wire pseudo-RE with greater biocompatibility.

3.5 Conclusion and Future Works

In this work, polarized IrOx pseudo-RE integrated Glu sensor is introduced for higher biocompatibility. By incorporating the RE into the sensor, the need for external RE is eliminated, which reduces the number of holes in the skull that need to be drilled for neurotransmitter measurements and enhances the overall stability of the sensing platform for freely behaving animal experiments. This can contribute to the increase in survival rate after neurotransmitter sensor implantation for long-term measurements *in vivo*. In addition, IrOx has been chosen as the RE material for less foreign body response and better biocompatibility compared to its AgCl counterpart. Furthermore, a way to better enhance the signal in terms of stability is introduced through surface polarization. However, although this chapter provides experimental results on the effect of polarization on IrOx film stability, further investigation on polarization of IrOx thin film in terms of chemical state change after polarization needs to be performed to better understand the mechanism.

Overall, real-time monitoring of neurotransmitters is an area of importance to reveal the pathways that lie behind neurological disorders. While many groups work on improving the sensor's performance in terms of sensitivity, selectivity, longevity, etc., a lot of times the biocompatibility is not as thoroughly investigated. This work demonstrates a highly biocompatible neurotransmitter sensor with IrOx incorporated RE that matches the performance of widely used pseudo-REs (Ag/AgCl wire pseudo-RE) for long-term *in vivo* neurotransmitter measurements. Our group is in the process of applying this polarized IrOx RE incorporated electrochemical sensor for simultaneous Glu and GABA recordings *in vivo* to look at the mechanism behind neurological diseases, such as autism spectrum disorder, Alzheimer's disease, stroke, etc.

3.6 Acknowledgements

The authors would like to acknowledge the financial support from the NSF CAREER Award #1917105 to H.C. and the NSF NCS Award #1926818 to H.C. and M.M.L.

CHAPTER 4: CONCLUSION AND FUTURE WORKS

4.1 Conclusion

The first half of this study focused on developing a flexible enzymatic electrochemical biosensor with high sensitivity for dual Glu:GABA detection. Electrodeposition of Pt-black and self-referencing technique was adopted to increase the sensitivity and SNR. Accordingly, Pt-black nanoparticle deposition's effect on increment of surface area has been shown with both SEM and electrochemical methods. Also, various combinations of metals were compared that showed Pt-black deposited Pt surface's superior oxidation properties towards H_2O_2. The resulting sensitivity and selectivity of the sensor for Glu and GABA has been demonstrated along with its longevity after fabrication. Moreover, the developed sensor has been thoroughly validated using various platforms including *in vitro*, *ex vivo* with neuronal cells and *in vivo* with rodent models. Then for the second half of this study, further improvements to the sensor have been made by increasing the biocompatibility of the sensor via incorporating IrOx pseudo-RE onto the electrode. To address the biocompatibility issue of commonly used Ag/AgCl wire pseudo-RE, IrOx has been explored as an alternative RE material. Moreover, we attempted to integrate the RE into the sensor by coating IrOx on one of the five pads on the probe. The IrOx coating was validated optically and using EDS. Furthermore, polarization has been introduced as a method to enhance the stability of the IrOx thin film. With the optimized polarized IrOx as a pseudo-RE, the performance of the sensor towards Glu has been tested against various REs. Altogether, a highly sensitive and biocompatible dual Glu:GABA sensor is proposed for aiding investigation of neurological disorders.

4.2 Future Works

The animal study for investigating neurological disorders using the proposed sensor has started through collaboration with several research labs. Specifically, our collaborators at Oregon Health & Science University (OHSU) with extensive knowledge and expertise in studying environmental factors that shape the social brain and behaviors relevant to autism using prairie voles are interested in exploring the change in Glu:GABA level resulting from ELSD. Unlike the common laboratory mice, prairie voles show a lot of social behaviors like human such as spending time with partners instead of an unfamiliar stranger and males taking part in raising the pub. This makes them an ideal animal model to study complex social behavior. So far, the preliminary data in Chapter 1 showing increased parvalbumin in the S1BF and increased population of dendritic spine around the PFC in ELSD subjects utilized immunohistochemistry and human observation, which further investigation was hindered due to technical limitations. The dual Glu:GABA electrochemical sensor developed in this work addresses this limitation by providing a method to measure Glu and GABA simultaneously during social interactions which has not been done for far. Our collaboration to explore continuous change in Glu and GABA levels in ELSD animals and during their social interactions has been initiated, where we are currently optimizing the experimental setup for at least 3-days continuous measurements during partner preference test. Another *in vivo* collaboration that we're working on is looking at Glu:GABA changes induced by stroke. Stroke occurs when blood flows to the brain is blocked of bleeding in the brain, where we expect Glu:GABA changes owing to the

disease. We hope to apply our sensor to investigate if there's any preceding neurotransmitter changes before stroke that can be used as a preventative measure. As a preliminary experiment, we tried inducing stroke in mouse with pilocorpine hydrochloride injection and measuring Glu level changes at hippocampus. As shown in Figure 4.1, our sensor was able to detect changes in Glu after drug injection and neurotransmitter burst from cells after death. With this preliminary result, we hope to further investigate neurological mechanisms behind stroke.

Further, despite the improvements that this work has made, there are still technical improvements that can be introduced to upgrade the biosensor system. One of the improvements that we have been working on is to make the sensor transparent. Since the sensor is intended to be implanted in the brain, if the sensor is transparent while maintaining its electrochemical functionality, it can further be integrated with optical

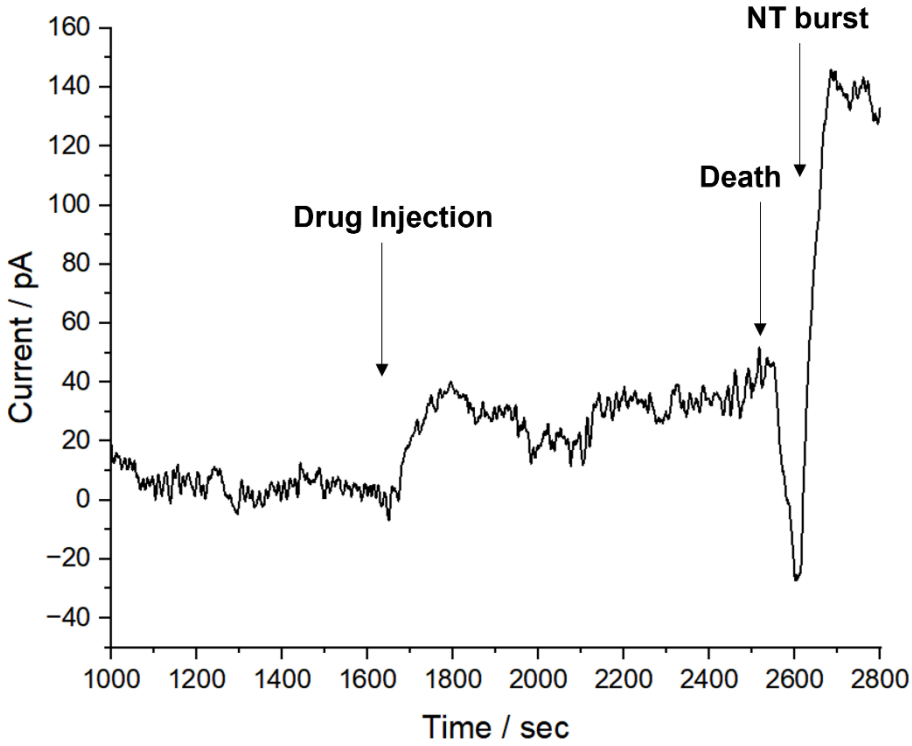

Figure 4.1 *In vivo L-glutamate recordings during stroke*

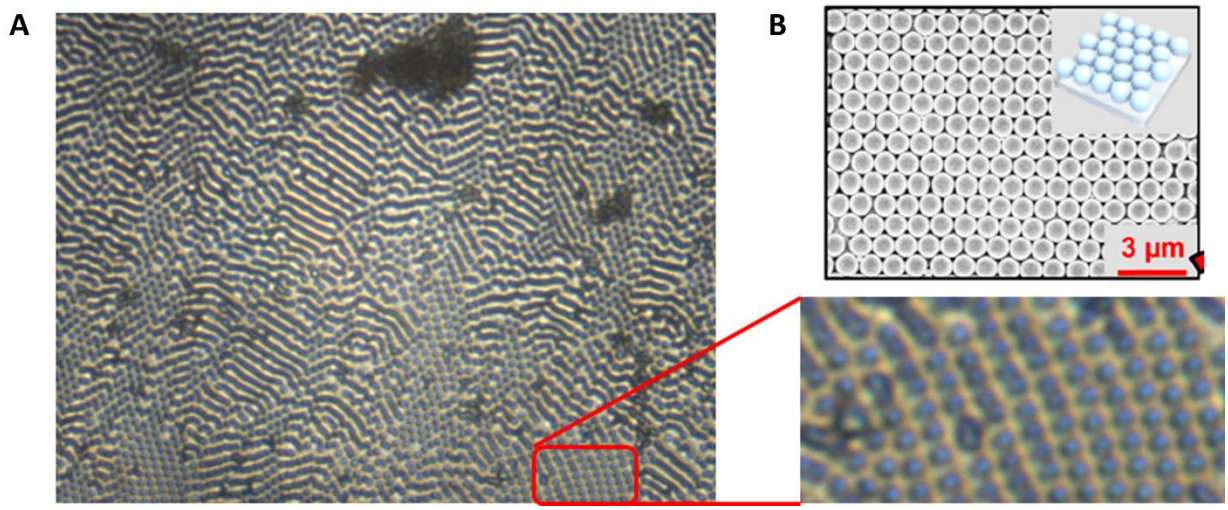

Figure 4.2 *(A) Polystyrene beads coated on glass substrate with enlarged image. (B) Ideal distribution of polystyrene beads.*

measurements to retract additional information. Currently, the substrate for our sensor is commercially available 5 MIL Kapton HN general-purpose polyimide film (125 µm) from DuPont. While it is transparent to some extent, when we deposit metal using electron beam, the plain layer of metal surface makes if fully opaque. Thus, if we can deposit metal in a way that can make the metal layer transparent, along with using fully transparent parylene C as a substrate, we'll be able to achieve an electrochemical sensor where light can pass that can be used for combined studies with optogenetics. Our lab has started investigating the possibility of using a metal nanomesh structure for transparent sensing electrode. Nanomesh refers to a structure that resembles an assembly of hexagonal pores with nanometer scale. If this structure is created with a metal layer, leaving the pores empty, the metals will still be connected for conduction but optically transparent due to the empty pores. There are several literatures on forming this structure using air-water interface, spin-coating, etc. and various methods are being tested to achieve a platinum nanomesh layer. The fabrication method that we're specifically exploring is forming a packed monolayer of polystyrene beads on the substrate using air-water interface and

spin-coating. By depositing metal on the monolayer of polystyrene beads, the metals will only be deposited at the gap between the beads forming a nanomesh structure. So far, as shown in Figure 4.2.B, we were able to form a monolayer of polystyrene beads using air-water interface. However, although there were some areas where we achieved a monolayer, the structure was not uniform. Also, aggregation of nanospheres was observed, which is not desired when forming a metal nanomesh layer. Therefore, we're also looking at using spin-coating as an alternative method. Currently, optics and electrochemistry are conducted separately, due to the lack of technology. However, integrating the two into one sensor along with on-probe light source will relieve the complication of inserting several sensors in the brain (Figure 4.3). Along with that, we also expect that the current flow in the nanomesh will differ with its unique structure. So, the sensor's sensitivity change from the structure will also be interesting to investigate for future directions.

Overall, several studies are ongoing with respect to the dual Glu:GABA sensor proposed in this dissertation. As the brain holds a lot of unexplored properties that many

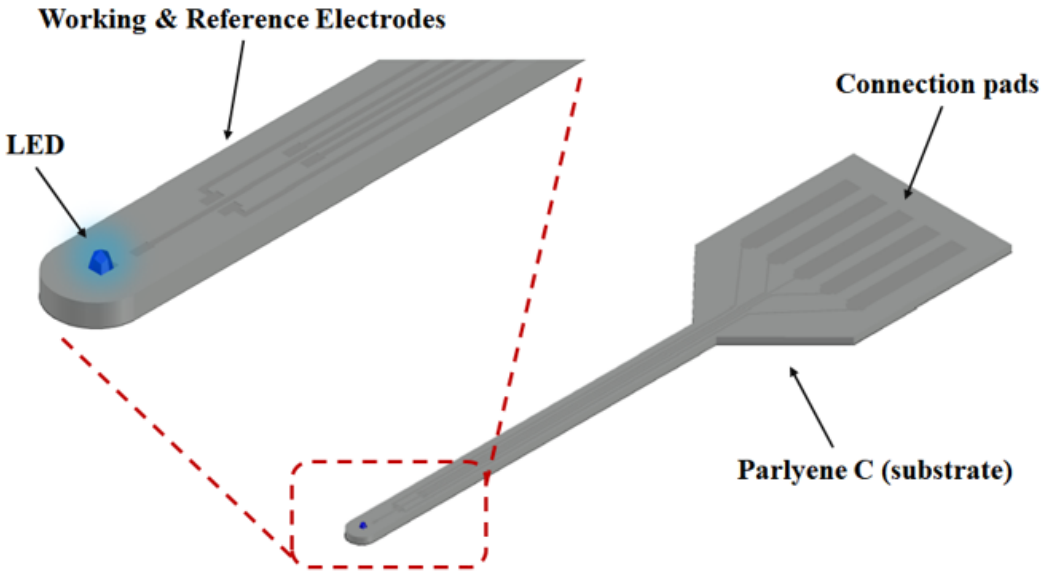

Figure 4.3 *Schematic design of transparent dual L-glutamate:GABA sensor with LED for optical stimulation*

groups are attempting to investigate, there are also various technical limitations that need to be addressed to perform animal experiments safely and effectively. In technical aspect, as mentioned multiple times, sensor characteristics such as sensitivity and selectivity need to be highly improved. The dual Glu:GABA sensor demonstrated here tries to address this by increasing the surface area of the electrode via electrochemical deposition of nanoparticles. However, to monitor the minute changes in neurotransmitters during social behaviors, higher sensitivity might be needed. Although this platform will be used to explore neurotransmitter levels *in vivo* with freely behaving animals to explore neurological disorders, if needed, modifying the 3D structure from nanoparticles to other structures such as nanopillars can be thought of to further enhance the surface area leading to even higher sensitivity. Also, adoption of conductive polymers as an additional layer can be another method of achieving higher sensitivity. As for the biological aspect, biocompatibility of the sensor needs to be highly improved. Here, integrating the RE into a single sensor and alternative material, IrOx, is suggested for the purpose. However, there's room for more improvements such as reducing the size of the sensor or coating an additional biocompatible layer to minimize the biofouling. As such, brain implantation of electrochemical sensors is a complicated procedure where thorough validation of the sensor platform and experimental setup need to be performed to execute effective and efficient long-term *in vivo* measurements. Although there are multiple hurdles that need to be overcome, this dissertation provides an initial step towards optimization and future directions for the field.

REFERENCES

[1] E. Anderzhanova and C. T. Wotjak, "Brain microdialysis and its applications in experimental neurochemistry," *Cell and tissue research,* vol. 354, pp. 27-39, 2013.

[2] J. Horder, M. M. Petrinovic, M. A. Mendez, A. Bruns, T. Takumi, W. Spooren*, et al.*, "Glutamate and GABA in autism spectrum disorder-a translational magnetic resonance spectroscopy study in man and rodent models," *Transl Psychiatry,* vol. 8, p. 106, May 25 2018.

[3] J. C. Klein, C. Eggers, E. Kalbe, S. Weisenbach, C. Hohmann, S. Vollmar*, et al.*, "Neurotransmitter changes in dementia with Lewy bodies and Parkinson disease dementia in vivo," *Neurology,* vol. 74, pp. 885-92, Mar 16 2010.

[4] D. M. Mann and P. O. Yates, "Pathological basis for neurotransmitter changes in Parkinson's disease," *Neuropathol Appl Neurobiol,* vol. 9, pp. 3-19, Jan-Feb 1983.

[5] D. C. Rojas, "The role of glutamate and its receptors in autism and the use of glutamate receptor antagonists in treatment," *J Neural Transm (Vienna),* vol. 121, pp. 891-905, Aug 2014.

[6] N. M. Rowley, K. K. Madsen, A. Schousboe, and H. Steve White, "Glutamate and GABA synthesis, release, transport and metabolism as targets for seizure control," *Neurochem Int,* vol. 61, pp. 546-58, Sep 2012.

[7] Z. Zhang, S. Zhang, P. Fu, Z. Zhang, K. Lin, J. K. Ko*, et al.*, "Roles of Glutamate Receptors in Parkinson's Disease," *Int J Mol Sci,* vol. 20, Sep 6 2019.

[8] Z. Zheng, T. Zhu, Y. Qu, and D. Mu, "Blood Glutamate Levels in Autism Spectrum Disorder: A Systematic Review and Meta-Analysis," *PLoS One,* vol. 11, p. e0158688, 2016.

[9] C. Lord, T. S. Brugha, T. Charman, J. Cusack, G. Dumas, T. Frazier*, et al.*, "Autism spectrum disorder," *Nat Rev Dis Primers,* vol. 6, p. 5, Jan 16 2020.

[10] W. H. Organization, "Autism spectrum disorders," World Health Organization. Regional Office for the Eastern Mediterranean2019.

[11] C. C. Fadini, D. A. Lamônica, A. C. Fett-Conte, E. Osório, G. M. Zuculo, C. M. Giacheti*, et al.*, "Influence of sleep disorders on the behavior of individuals with autism spectrum disorder," *Frontiers in Human Neuroscience,* vol. 9, p. 347, 2015.

[12] K. S. Turner and C. R. Johnson, "Behavioral interventions to address sleep disturbances in children with autism spectrum disorders: A review," *Topics in Early Childhood Special Education,* vol. 33, pp. 144-152, 2013.

[13] M. E. Verhoeff, L. M. Blanken, D. Kocevska, V. R. Mileva-Seitz, V. W. Jaddoe, T. White*, et al.*, "The bidirectional association between sleep problems and autism spectrum disorder: a population-based cohort study," *Molecular Autism,* vol. 9, pp. 1-9, 2018.

[14] A. S. Darvesh, R. T. Carroll, W. J. Geldenhuys, G. A. Gudelsky, J. Klein, C. K. Meshul*, et al.*, "In vivo brain microdialysis: advances in neuropsychopharmacology and drug discovery," *Expert opinion on drug discovery,* vol. 6, pp. 109-127, 2011.

[15] R. Nirogi, K. Mudigonda, V. Kandikere, and R. Ponnamaneni, "Quantification of acetylcholine, an essential neurotransmitter, in brain microdialysis samples by liquid chromatography mass spectrometry," *Biomedical Chromatography,* vol. 24, pp. 39-48, 2010.

[16] J. Zhang, A. Jaquins-Gerstl, K. M. Nesbitt, S. C. Rutan, A. C. Michael, and S. G. Weber, "In vivo monitoring of serotonin in the striatum of freely moving rats with one minute temporal resolution by online microdialysis–capillary high-performance liquid chromatography at elevated temperature and pressure," *Analytical chemistry,* vol. 85, pp. 9889-9897, 2013.

[17] B. Si and E. Song, "Recent advances in the detection of neurotransmitters," *Chemosensors,* vol. 6, p. 1, 2018.

[18] Z. Tavakolian-Ardakani, O. Hosu, C. Cristea, M. Mazloum-Ardakani, and G. Marrazza, "Latest trends in electrochemical sensors for neurotransmitters: A review," *Sensors,* vol. 19, p. 2037, 2019.
[19] H. Kaur, S. S. Siwal, R. V. Saini, N. Singh, and V. K. Thakur, "Significance of an Electrochemical Sensor and Nanocomposites: Toward the Electrocatalytic Detection of Neurotransmitters and Their Importance within the Physiological System," *ACS Nanoscience Au,* vol. 3, pp. 1-27, 2022.
[20] S. D. Niyonambaza, P. Kumar, P. Xing, J. Mathault, P. De Koninck, E. Boisselier*, et al.*, "A review of neurotransmitters sensing methods for neuro-engineering research," *Applied Sciences,* vol. 9, p. 4719, 2019.
[21] S. Durairaj, B. Sidhureddy, J. Cirone, and A. Chen, "Nanomaterials-based electrochemical sensors for in vitro and in vivo analyses of neurotransmitters," *Applied sciences,* vol. 8, p. 1504, 2018.
[22] Z. Fredj, B. Singh, M. Bahri, P. Qin, and M. Sawan, "Enzymatic Electrochemical Biosensors for Neurotransmitters Detection: Recent Achievements and Trends," *Chemosensors,* vol. 11, p. 388, 2023.
[23] M. Shen and M. L. Colombo, "Electrochemical nanoprobes for the chemical detection of neurotransmitters," *Analytical Methods,* vol. 7, pp. 7095-7105, 2015.
[24] B. Harris, M. B. McClain, S. Schwartz, and C. R. Haverkamp, "Knowledge of autism spectrum disorder among school psychology graduate students," *Contemporary School Psychology,* vol. 24, pp. 239-247, 2020.
[25] J. J. Hutsler and H. Zhang, "Increased dendritic spine densities on cortical projection neurons in autism spectrum disorders," *Brain research,* vol. 1309, pp. 83-94, 2010.
[26] M. Milovanovic and R. Grujicic, "Electroencephalography in assessment of autism spectrum disorders: a review," *Frontiers in psychiatry,* vol. 12, p. 686021, 2021.
[27] T. Chomiak, V. Karnik, E. Block, and B. Hu, "Altering the trajectory of early postnatal cortical development can lead to structural and behavioural features of autism," *BMC neuroscience,* vol. 11, pp. 1-10, 2010.
[28] I. M. Trutzer, M. Á. García-Cabezas, and B. Zikopoulos, "Postnatal development and maturation of layer 1 in the lateral prefrontal cortex and its disruption in autism," *Acta neuropathologica communications,* vol. 7, pp. 1-23, 2019.
[29] C. Jones, R. Olson, A. Chau, P. Wickham, R. Leriche, C. Reynolds*, et al.*, "025 Sleep Disruption on an Orbital Shaker alters Glutamate in Prairie Vole Prefrontal Cortex," *Sleep,* vol. 44, pp. A11-A12, 2021.
[30] C. E. Jones, A. Q. Chau, R. J. Olson, C. Moore, P. T. Wickham, N. Puranik*, et al.*, "Early life sleep disruption alters glutamate and dendritic spines in prefrontal cortex and impairs cognitive flexibility in prairie voles," *Current research in neurobiology,* vol. 2, p. 100020, 2021.
[31] K. N. Hascup, E. C. Rutherford, J. E. Quintero, B. K. Day, J. R. Nickell, F. Pomerleau*, et al.*, "Second-by-second measures of L-glutamate and other neurotransmitters using enzyme-based microelectrode arrays," *Electrochemical methods for neuroscience,* 2007.
[32] S. S. Chu, H. A. Nguyen, J. Zhang, S. Tabassum, and H. Cao, "Towards Multiplexed and Multimodal Biosensor Platforms in Real-Time Monitoring of Metabolic Disorders," *Sensors,* vol. 22, p. 5200, 2022.
[33] S. Baluta, D. Zając, A. Szyszka, K. Malecha, and J. Cabaj, "Enzymatic platforms for sensitive neurotransmitter detection," *Sensors,* vol. 20, p. 423, 2020.
[34] S. Chandra, S. Siraj, and D. K. Wong, "Recent advances in biosensing for neurotransmitters and disease biomarkers using microelectrodes," *ChemElectroChem,* vol. 4, pp. 822-833, 2017.
[35] S. Billa, Y. Yanamadala, I. Hossain, S. Siddiqui, N. Moldovan, T. A. Murray*, et al.*, "Brain-implantable multifunctional probe for simultaneous detection of glutamate and GABA neurotransmitters: optimization and in vivo studies," *Micromachines,* vol. 13, p. 1008, 2022.

[36] Z. Li, Y. Song, G. Xiao, F. Gao, S. Xu, M. Wang*, et al.*, "Bio-electrochemical microelectrode arrays for glutamate and electrophysiology detection in hippocampus of temporal lobe epileptic rats," *Analytical biochemistry,* vol. 550, pp. 123-131, 2018.

[37] N. Moldovan, I.-I. Blaga, S. Billa, I. Hossain, C. Gong, C. E. Jones*, et al.*, "Brain-implantable multifunctional probe for simultaneous detection of glutamate and GABA neurotransmitters," *Sensors and Actuators B: Chemical,* vol. 337, p. 129795, 2021.

[38] J. L. Scoggin, C. Tan, N. H. Nguyen, U. Kansakar, M. Madadi, S. Siddiqui*, et al.*, "An enzyme-based electrochemical biosensor probe with sensitivity to detect astrocytic versus glioma uptake of glutamate in real time in vitro," *Biosensors and Bioelectronics,* vol. 126, pp. 751-757, 2019.

[39] R. M. Guerriero, C. C. Giza, and A. Rotenberg, "Glutamate and GABA Imbalance Following Traumatic Brain Injury," *Current Neurology and Neuroscience Reports,* vol. 15, May 2015.

[40] M. A. Kurian, P. Gissen, M. Smith, S. J. R. Heales, and P. T. Clayton, "The monoamine neurotransmitter disorders: an expanding range of neurological syndromes," *Lancet Neurology,* vol. 10, pp. 721-733, Aug 2011.

[41] D. L. Robinson, A. Hermans, A. T. Seipel, and R. M. Wightman, "Monitoring rapid chemical communication in the brain," *Chemical Reviews,* vol. 108, pp. 2554-2584, Jul 2008.

[42] S. G. Sandberg and P. A. Garris, "Neurochemistry of Addiction Monitoring Essential Neurotransmitters of Addiction," *Advances in the Neuroscience of Addiction,* pp. 99-135, 2010.

[43] M. J. Maenner, K. A. Shaw, A. V. Bakian, D. A. Bilder, M. S. Durkin, A. Esler*, et al.*, "Prevalence and Characteristics of Autism Spectrum Disorder Among Children Aged 8 Years - Autism and Developmental Disabilities Monitoring Network, 11 Sites, United States, 2018," *Mmwr Surveillance Summaries,* vol. 70, Dec 3 2021.

[44] A. El-Ansary and L. Al-Ayadhi, "GABAergic/glutamatergic imbalance relative to excessive neuroinflammation in autism spectrum disorders," *Journal of Neuroinflammation,* vol. 11, Nov 19 2014.

[45] R. Gao and P. Penzes, "Common Mechanisms of Excitatory and Inhibitory Imbalance in Schizophrenia and Autism Spectrum Disorders," *Current Molecular Medicine,* vol. 15, pp. 146-167, 2015.

[46] C. E. Jones, A. Q. Chau, R. J. Olson, C. Moore, P. T. Wickham, N. Puranik*, et al.*, "Early life sleep disruption alters glutamate and dendritic spines in prefrontal cortex and impairs cognitive flexibility in prairie voles," *Curr Res Neurobiol,* vol. 2, 2021.

[47] C. E. Jones, R. A. Opel, M. E. Kaiser, A. Q. Chau, J. R. Quintana, M. A. Nipper*, et al.*, "Early-life sleep disruption increases parvalbumin in primary somatosensory cortex and impairs social bonding in prairie voles," *Sci Adv,* vol. 5, p. eaav5188, Jan 2019.

[48] C. E. Jones, P. T. Wickham, and M. M. Lim, "Early Life Sleep Disruption Is a Risk Factor for Increased Ethanol Drinking After Acute Footshock Stress in Prairie Voles," *Behavioral Neuroscience,* vol. 134, pp. 424-434, Oct 2020.

[49] C. Defaix, A. Solgadi, T. H. Pham, A. M. Gardier, P. Chaminade, and L. Tritschler, "Rapid analysis of glutamate, glutamine and GABA in mice frontal cortex microdialysis samples using HPLC coupled to electrospray tandem mass spectrometry," *Journal of Pharmaceutical and Biomedical Analysis,* vol. 152, pp. 31-38, Apr 15 2018.

[50] N. J. Reinhoud, H. J. Brouwer, L. M. van Heerwaarden, and G. A. H. Korte-Bouws, "Analysis of Glutamate, GABA, Noradrenaline, Dopamine, Serotonin, and Metabolites Using Microbore UHPLC with Electrochemical Detection," *Acs Chemical Neuroscience,* vol. 4, pp. 888-894, May 2013.

[51] L. Denoroy and S. Parrot, "Biochemical Approaches for Glutamatergic Neurotransmission Preface," *Biochemical Approaches for Glutamatergic Neurotransmission,* vol. 130, pp. Vii-Viii, 2018.

[52] R. A. Saylor, S. R. Thomas, and S. M. Lunte, "Separation-based methods combined with microdialysis sampling for monitoring neurotransmitters and drug delivery to the brain," in *COMPENDIUM OF IN VIVO MONITORING IN REAL-TIME MOLECULAR NEUROSCIENCE: Volume 2: Microdialysis and Sensing of Neural Tissues*, ed, 2017, pp. 1-45.

[53] G. E. Fenoy, W. A. Marmisolle, O. Azzaroni, and W. Knoll, "Acetylcholine biosensor based on the electrochemical functionalization of graphene field-effect transistors," *Biosensors & Bioelectronics,* vol. 148, Jan 15 2020.

[54] E. A. Kiyatkin and K. T. Wakabayashi, "Parsing Glucose Entry into the Brain: Novel Findings Obtained with Enzyme-Based Glucose Biosensors," *Acs Chemical Neuroscience,* vol. 6, pp. 108-116, Jan 2015.

[55] Y. Q. Lin, P. Yu, J. Hao, Y. X. Wang, T. Ohsaka, and L. Q. Mao, "Continuous and Simultaneous Electrochemical Measurements of Glucose, Lactate, and Ascorbate in Rat Brain Following Brain Ischemia," *Analytical Chemistry,* vol. 86, pp. 3895-3901, Apr 15 2014.

[56] C. B. Liu, Y. Zhao, X. Cai, Y. Xie, T. Y. Wang, D. L. Cheng*, et al.*, "A wireless, implantable optoelectrochemical probe for optogenetic stimulation and dopamine detection," *Microsystems & Nanoengineering,* vol. 6, Aug 24 2020.

[57] K. A. Alamry, M. A. Hussein, J. W. Choi, and W. A. El-Said, "Non-enzymatic electrochemical sensor to detect gamma-aminobutyric acid with ligand-based on graphene oxide modi fied gold electrode," *Journal of Electroanalytical Chemistry,* vol. 879, Dec 15 2020.

[58] M. Ganesana, E. Trikantzopoulos, Y. Maniar, S. T. Lee, and B. J. Venton, "Development of a novel micro biosensor for in vivo monitoring of glutamate release in the brain," *Biosensors & Bioelectronics,* vol. 130, pp. 103-109, Apr 1 2019.

[59] X. M. Wen, B. Wang, S. Huang, T. Y. Liu, M. S. Lee, P. S. Chung*, et al.*, "Flexible, multifunctional neural probe with liquid metal enabled, ultra-large tunable stiffness for deep-brain chemical sensing and agent delivery," *Biosensors & Bioelectronics,* vol. 131, pp. 37-45, Apr 15 2019.

[60] J. J. Burmeister, D. A. Price, F. Pomerleau, P. Huettl, J. E. Quintero, and G. A. Gerhardt, "Challenges of simultaneous measurements of brain extracellular GABA and glutamate in vivo using enzyme-coated microelectrode arrays," *J Neurosci Methods,* vol. 329, p. 108435, Jan 1 2020.

[61] I. Hossain, C. Tan, P. T. Doughty, G. Dutta, T. A. Murray, S. Siddiqui*, et al.*, "A Novel Microbiosensor Microarray for Continuous ex Vivo Monitoring of Gamma-Aminobutyric Acid in Real-Time," *Front Neurosci,* vol. 12, p. 500, 2018.

[62] N. Moldovan, Blaga, II, S. Billa, I. Hossain, C. Gong, C. E. Jones*, et al.*, "Brain-Implantable Multifunctional Probe for Simultaneous Detection of Glutamate and GABA Neurotransmitters," *Sens Actuators B Chem,* vol. 337, Jun 15 2021.

[63] S. Billa, Y. Yanamadala, I. Hossain, S. Siddiqui, N. Moldovan, T. A. Murray*, et al.*, "Brain-Implantable Multifunctional Probe for Simultaneous Detection of Glutamate and GABA Neurotransmitters: Optimization and In Vivo Studies," *Micromachines,* vol. 13, Jul 2022.

[64] P. T. Doughty, I. Hossain, C. G. Gong, K. A. Ponder, S. Pati, P. U. Arumugam*, et al.*, "Novel microwire-based biosensor probe for simultaneous real-time measurement of glutamate and GABA dynamics in vitro and in vivo," *Scientific Reports,* vol. 10, Jul 29 2020.

[65] N. Wahono, S. Qin, P. Oomen, T. I. F. Cremers, M. G. de Vries, and B. H. C. Westerink, "Evaluation of permselective membranes for optimization of intracerebral amperometric glutamate biosensors," *Biosensors & Bioelectronics,* vol. 33, pp. 260-266, Mar 15 2012.

[66] D. M. Zhou, Y. Q. Dai, and K. K. Shiu, "Poly(phenylenediamine) film for the construction of glucose biosensors based on platinized glassy carbon electrode," *Journal of Applied Electrochemistry,* vol. 40, pp. 1997-2003, Nov 2010.

[67] M. Zaib and M. M. Athar, "Electrochemical characterization of a Porphyridium cruentum-modified carbon paste electrode by cyclic voltammetry," *Instrumentation Science & Technology,* vol. 46, pp. 408-425, 2018.
[68] B. Rezaei and N. Irannejad, "Electrochemical detection techniques in biosensor applications," in *Electrochemical biosensors*, ed: Elsevier, 2019, pp. 11-43.
[69] S. S. Chu, P. Marsh, H. A. Nguyen, C. E. Jones, M. M. Lim, and H. Cao, "Fabrication of Highly Sensitive Pt-black Electrochemical Sensors for GABA Detection," *2021 43rd Annual International Conference of the Ieee Engineering in Medicine & Biology Society (Embc),* pp. 7148-7151, 2021.
[70] S. S. Chu, P. Marsh, H. A. Nguyen, R. Olson, C. E. Jones, M. M. Lim*, et al.*, "Facile Fabrication of Highly Sensitive Pt-Black Electrochemical Sensor for L-Glutamate Detection," *2021 34th Ieee International Conference on Micro Electro Mechanical Systems (Mems 2021),* pp. 551-554, 2021.
[71] S. K. Hamdan and Z. M. Zain, "In vivo Electrochemical Biosensor for Brain Glutamate Detection: A Mini Review," *Malaysian Journal of Medical Sciences,* vol. 21, pp. 12-26, Dec 2014.
[72] H. Cao, A. L. Li, C. M. Nguyen, Y. B. Peng, and J. C. Chiao, "An Integrated Flexible Implantable Micro-Probe for Sensing Neurotransmitters," *Ieee Sensors Journal,* vol. 12, pp. 1618-1624, May 2012.
[73] F. T. C. Moreira, M. G. F. Sale, and M. Di Lorenzo, "Towards timely Alzheimer diagnosis: A self-powered amperometric biosensor for the neurotransmitter acetylcholine," *Biosensors & Bioelectronics,* vol. 87, pp. 607-614, Jan 15 2017.
[74] Y. G. Ou, A. M. Buchanan, C. E. Witt, and P. Hashemi, "Frontiers in electrochemical sensors for neurotransmitter detection: towards measuring neurotransmitters as chemical diagnostics for brain disorders," *Analytical Methods,* vol. 11, pp. 2738-2755, Jun 6 2019.
[75] A. Weltin, J. Kieninger, and G. A. Urban, "Microfabricated, amperometric, enzyme-based biosensors for in vivo applications," *Analytical and Bioanalytical Chemistry,* vol. 408, pp. 4503-4521, Jul 2016.
[76] J. L. He, G. Oeltzschner, M. Mikkelsen, A. Deronda, A. D. Harris, D. Crocetti*, et al.*, "Region-specific elevations of glutamate plus glutamine correlate with the sensory symptoms of autism spectrum disorders," *Translational Psychiatry,* vol. 11, Jul 29 2021.
[77] V. O. Manyukhina, A. O. Prokofyev, I. A. Galuta, D. E. Goiaeva, T. S. Obukhova, J. F. Schneiderman*, et al.*, "Globally elevated excitation-inhibition ratio in children with autism spectrum disorder and below-average intelligence," *Molecular Autism,* vol. 13, May 12 2022.
[78] H. S. Zhao, X. J. Mao, C. L. Zhu, X. H. Zou, F. Z. Peng, W. Yang*, et al.*, "GABAergic System Dysfunction in Autism Spectrum Disorders," *Frontiers in Cell and Developmental Biology,* vol. 9, Feb 7 2022.
[79] M. Nimgampalle, H. Chakravarthy, S. Sharma, S. Shree, A. R. Bhat, J. A. Pradeepkiran*, et al.*, "Neurotransmitter systems in the etiology of major neurological disorders: Emerging insights and therapeutic implications," *Ageing Res Rev,* vol. 89, p. 101994, Aug 2023.
[80] R. Liu, Z.-Y. Feng, D. Li, B. Jin, Y. Lan, and L.-Y. Meng, "Recent trends in carbon-based microelectrodes as electrochemical sensors for neurotransmitter detection: A review," *TrAC Trends in Analytical Chemistry,* vol. 148, p. 116541, 2022.
[81] Z. Tavakolian-Ardakani, O. Hosu, C. Cristea, M. Mazloum-Ardakani, and G. Marrazza, "Latest Trends in Electrochemical Sensors for Neurotransmitters: A Review," *Sensors (Basel),* vol. 19, Apr 30 2019.
[82] Y. Ou, A. M. Buchanan, C. E. Witt, and P. Hashemi, "Frontiers in electrochemical sensors for neurotransmitter detection: towards measuring neurotransmitters as chemical diagnostics for brain disorders," *Analytical Methods,* vol. 11, pp. 2738-2755, 2019.
[83] S. Billa, Y. Yanamadala, I. Hossain, S. Siddiqui, N. Moldovan, T. A. Murray*, et al.*, "Brain-Implantable Multifunctional Probe for Simultaneous Detection of Glutamate and GABA

Neurotransmitters: Optimization and In Vivo Studies," *Micromachines (Basel),* vol. 13, Jun 26 2022.
[84] R. G. Krishnan and B. Saraswathyamma, "Murexide-derived in vitro electrochemical sensor for the simultaneous determination of neurochemicals," *Anal Bioanal Chem,* vol. 413, pp. 6803-6812, Nov 2021.
[85] N. Lavanya and C. Sekar, "Electrochemical sensor for simultaneous determination of epinephrine and norepinephrine based on cetyltrimethylammonium bromide assisted SnO2 nanoparticles," *Journal of Electroanalytical Chemistry,* vol. 801, pp. 503-510, 2017.
[86] R. K. Franklin, M. D. Johnson, K. A. Scott, J. H. Shim, H. Nam, D. R. Kipke*, et al.*, "Iridium oxide reference electrodes for neurochemical sensing with MEMS microelectrode arrays," *2005 Ieee Sensors, Vols 1 and 2,* pp. 1400-1403, 2005.
[87] F. Ribet, G. Stemme, and N. Roxhed, "Ultra-miniaturization of a planar amperometric sensor targeting continuous intradermal glucose monitoring," *Biosens Bioelectron,* vol. 90, pp. 577-583, Apr 15 2017.
[88] B. T. Seaton and M. L. Heien, "Biocompatible reference electrodes to enhance chronic electrochemical signal fidelity in vivo," *Anal Bioanal Chem,* vol. 413, pp. 6689-6701, Nov 2021.
[89] B. Wang, L. Feng, B. Koo, and H. G. Monbouquette, "A Complete Electroenzymatic Choline Microprobe Based on Nanostructured Platinum Microelectrodes and an IrOx On-probe Reference Electrode," *Electroanalysis,* vol. 31, pp. 1249-1253, 2019.
[90] S. R. Ng and D. O'Hare, "An iridium oxide microelectrode for monitoring acute local pH changes of endothelial cells," *Analyst,* vol. 140, pp. 4224-31, Jun 21 2015.
[91] J. Rouhi, S. Kakooei, M. C. Ismail, R. Karimzadeh, and M. R. Mahmood, "Development of iridium oxide sensor for surface pH measurement of a corroding metal under deposit," *International Journal of Electrochemical Science,* vol. 12, pp. 9933-9943, 2017.
[92] A. Salimi, V. Alizadeh, and R. G. Compton, "Disposable amperometric sensor for neurotransmitters based on screen-printed electrodes modified with a thin iridium oxide film," *Anal Sci,* vol. 21, pp. 1275-80, Nov 2005.
[93] K. Yamanaka, "Anodically electrodeposited iridium oxide films (AEIROF) from alkaline solutions for electrochromic display devices," *Japanese journal of applied physics,* vol. 28, p. 632, 1989.
[94] S. Kakooei, M. C. Ismail, and B. Ari-Wahjoedi, "An overview of pH sensors based on iridium oxide: fabrication and application," *Int. J. Mater. Sci. Innov,* vol. 1, pp. 62-72, 2013.
[95] S. Mahmoud, A. Riad, M. El-Deeb, and T. B. Nasrallah, "Influence of Some Preparative Parameters on Microstructure and Electrochromic Behavior of Sprayed Iridium Oxide Films," *International Journal of Applied Physics and Mathematics,* vol. 3, p. 381, 2013.
[96] C. M. Nguyen, S. Rao, X. Yang, S. Dubey, J. Mays, H. Cao*, et al.*, "Sol-gel deposition of iridium oxide for biomedical micro-devices," *Sensors (Basel),* vol. 15, pp. 4212-28, Feb 12 2015.
[97] M. Nedergaard, R. Kraig, J. Tanabe, and W. Pulsinelli, "Dynamics of interstitial and intracellular pH in evolving brain infarct," *American Journal of Physiology-Regulatory, Integrative and Comparative Physiology,* vol. 260, pp. R581-R588, 1991.
[98] W.-D. Huang, H. Cao, S. Deb, M. Chiao, and J.-C. Chiao, "A flexible pH sensor based on the iridium oxide sensing film," *Sensors and Actuators A: Physical,* vol. 169, pp. 1-11, 2011.
[99] S. Carroll and R. P. Baldwin, "Self-calibrating microfabricated iridium oxide pH electrode array for remote monitoring," *Analytical chemistry,* vol. 82, pp. 878-885, 2010.
[100] W. Olthuis, M. Robben, P. Bergveld, M. Bos, and W. Van der Linden, "pH sensor properties of electrochemically grown iridium oxide," *Sensors and Actuators B: Chemical,* vol. 2, pp. 247-256, 1990.